

## Article

# The Electrodeposition of Derivatives of Pyrrole and Thiophene on Brass Alloy in the Presence of Dodecane-1-Sulfonic Acid Sodium Salt in Acidic Medium and Its Anti-Corrosive Properties

Florina Branzoi \* and Simona Petrescu

Institute of Physical Chemistry "Ilie Murgulescu", 202 Splaiul Independenței, 060021 Bucharest, Romania

\* Correspondence: fbranzoi@chimfiz.icf.ro

**Abstract:** In this paper, potentiostatic and galvanostatic deposition (electrochemical deposition) processes have been used for the obtained of a new composite polymer: N-methylpyrrole-sodium 1-dodecanesulfonate/poly 2-methylthiophene (PNMPY-1SSD/P2MT) coatings over brass electrode for corrosion protection. The sodium 1-dodecanesulfonate as a dopant ion employed in the electropolymerization procedure can have a meaningful effect on the anti-corrosion protection of the composite polymeric film by stopping the penetration of corrosive ions. The composite coatings have been characterized by cyclic voltammetry, Fourier transform infrared (FT-IR) spectroscopy, and scanning electron microscopy (SEM) procedures. The anti-corrosion performance of PNMPY-1SSD/P2MT coated brass has been investigated by potentiostatic and potentiodynamic polarization and electrochemical impedance spectroscopy (EIS) practices in 0.5 M H<sub>2</sub>SO<sub>4</sub> medium. The corrosion assessment of PNMPY-1SSD/P2MT coated brass was noticed to be ~9 times diminished than of uncoated brass, and the efficiency of these protective coatings of this coating is above 90%. The highest effectiveness is realized by the electrochemical deposition of PNMPY-1SSD/P2MT obtained at 1.1 V and 1.4 V potential applied and at 0.5 mA/cm<sup>2</sup> and 1 mA/cm<sup>2</sup> current densities applied in molar ratio 5:3. The outcomes of the corrosion tests denoted that PNMPY-1SSD/P2MT coatings assure good anti-corrosion protection of brass in corrosive media.

**Keywords:** conducting polymer; electropolymerization; corrosion protection; brass; coating; EIS; SEM



**Citation:** Branzoi, F.; Petrescu, S. The Electrodeposition of Derivatives of Pyrrole and Thiophene on Brass Alloy in the Presence of Dodecane-1-Sulfonic Acid Sodium Salt in Acidic Medium and Its Anti-Corrosive Properties. *Coatings* **2023**, *13*, 953. <https://doi.org/10.3390/coatings13050953>

Academic Editor: Heping Li

Received: 26 April 2023

Revised: 11 May 2023

Accepted: 16 May 2023

Published: 19 May 2023



**Copyright:** © 2023 by the authors. Licensee MDPI, Basel, Switzerland. This article is an open access article distributed under the terms and conditions of the Creative Commons Attribution (CC BY) license (<https://creativecommons.org/licenses/by/4.0/>).

## 1. Introduction

The development of protective coatings of conducting polymers on active metals is one of the on a wide scale elaborated area in the domain of corrosion protection [1–5]. Organic coatings are repeatedly utilized to protect these metals and their alloys from corrosion. At present, conducting polymers have acquired meaningful interest, for example, protective coatings for varied metals and their alloys, because the main action of these composite coatings is to behave as a barrier for the corrosive agents [5–9]. This behavior can be perfected by achieving organic coatings, which have an important application in diverse domains of materials that are plain to attain and pliable to start at a large range. It was established that the electrochemical and physical features of polymers are notably affected by the type of dopant and electrolyte regarding the electrodeposition procedure. In recent years, conducting polymers has attracted considerable attentiveness in scientific and technological domains in agreement with their chemical, environmental, biological, electrical, thermal, and optical characteristics, the ease of their obtaining, and their wide applications. Brass is an alloy (Cu–Zn) frequently employed in nearly all industries for practical or esthetic scopes. Brass materials own interesting properties specifically, good physical properties, mechanical strength, high thermal and electrical conductivity, and higher resistance to biofouling. Brass is utilized in some industrial practices, such as automotive, electronics, fuel gas, water

distribution devices, water treating oneness, condensers, desalination, telecommunications, and marine. This material is sensitive to atmospheric corrosion, which was the theme of several examinations to defend them. While the effect of the environment and numerous chemicals may be insignificant, in corrosive environments, brass is susceptible to corrosion. Some investigators have explored brass corrosion [6–9]. Several procedures are utilized to enhance the anti-corrosion endurance of the brass employed like mechanical pieces in manufacture. The application of inhibitors, using organic, metallic or inorganic coverings, cathodic and anodic defense, electrochemical polymerization method, and nanostructure coating are techniques for metallic materials anti-corrosion protection [7–12]. Corrosion of metallic materials divulges a considerable economic and manufacturing (technological) concern. In technological practices, the metal areas employed are exhibited to greatly corrosive acids and basis media that cause significant corrosion and damage. In consequence, the goals of electrodeposition of these coatings on varied metals and establishing their corrosion defense characteristics have taken to rising attention. While corrosion is a significant part of the destruction of manufacturing structures, a large number of investigations were accomplished to find procedures to diminish corrosion and “wear costs”. Sulfuric acid solutions are employed in a number of technological processes that currently cause severe metallic corrosion of varied metal structures and equipment in manufacturing environments. Some examinations carried out for the protection of metallic materials in the zone of engineering have determined that composite coatings are utilized as the most efficacious and plain way to hinder the deterioration of these materials in corrosive media [11–17]. In addition, the rate of corrosion that the metallic materials display in an acidic solution is greatly raised, mainly when soluble corrosion results are acquired. The composite materials obtained from conducting polymers have a number of specific features, also improved chemical steadfastness, thermostability, favorable to the environment, and appropriate barrier provided [17–21]. Conducting polymers such as polyaniline, polypyrrole, polythiophene, and their derivatives are the most currently employed for protecting coverings [22–32]. Therefore, the incorporation of hydrophobic functionary groups is supposed to raise the polymer protection ability. The dopant ions incorporated into conducting polymers exercise an impact on both the electropolymerization procedure and the features of the acquired polymeric composites [33–38]. The dopant ion used by electrochemical deposition can have a significant effect on the ion-exchange selectiveness numeral of conducting polymers. In several events, the integration of larger hydrophobic dopant ions, e.g., anionic surfactant, arises in the formation of a polymer effective for cation exchange with completely hydrophobic characteristics [38–42]. As an example, the methylpyrrole-methylthiophene coating electrochemical synthesized from a solution including the 1SSD– 1dodecanesulfonate) dopant ion is permeable only to cations, and therefore, aggressive ions retard the touching of the polymer film sample surface. Hence, the utilization of this dopant throughout the electropolymerization of monomers assures a considerable diminution in the corrosion rate of metallic materials [40–43].

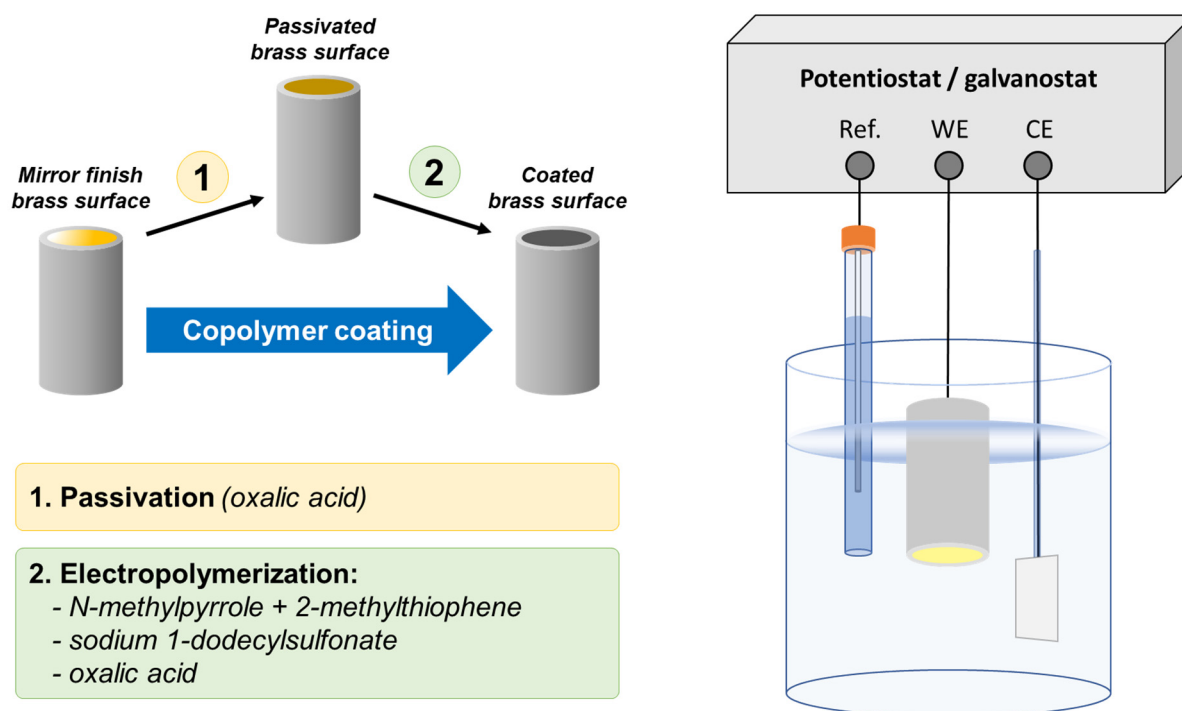
The aim of this research is to achieve new conductive polymers proper for the anti-corrosion defense of usual metals. Additionally, expanding appropriate electrochemical polymerization procedures that will offer the capacity to acquire dense, uniform, good-adhesion composite coatings on metallic electrodes. Another focus zone is attaining and optimizing new composite polymers of the best anti-corrosion estates for some metallic materials in corrosive environments. These new composite coatings are distinct from those related to the specialty literature and accomplish higher experimental results. This paper implicates the electrochemical synthesis and spectroscopic and electrochemical exploration of the novel composite poly (N-methylpyrrole-sodium 1-dodecanesulfonate/ 2 methylthiophene) and the corrosion compartment of this new coatings. This inquiry is a continuance of previous papers on attain and the assessment of some composite coating adequate for the protection of the metals and their alloys versus corrosion in corrosive media. The new composite material (PNMPY-1-SSD/P2MT) was electrodeposited onto brass substrate by potentiostatic and galvanostatic process from solutions of synthesis of 0.1 M

N-methylpyrrole, 0.1 M 2-methylthiophene, and 0.02 M sodium 1-dodecanesulfonate and 0.3 M oxalic acid. The analysis of the new coatings has been achieved by cyclic voltammetry, Fourier transform infrared (FT-IR) spectroscopy, and scanning electron microscopy (SEM) practices. Corrosion determinations of PPMPY-1-SSD/P2MT-covered brass were considered by potentiostatic and potentiodynamic polarization and electrochemical impedance spectroscopy (EIS) practices in 0.5 M sulfuric acid medium.

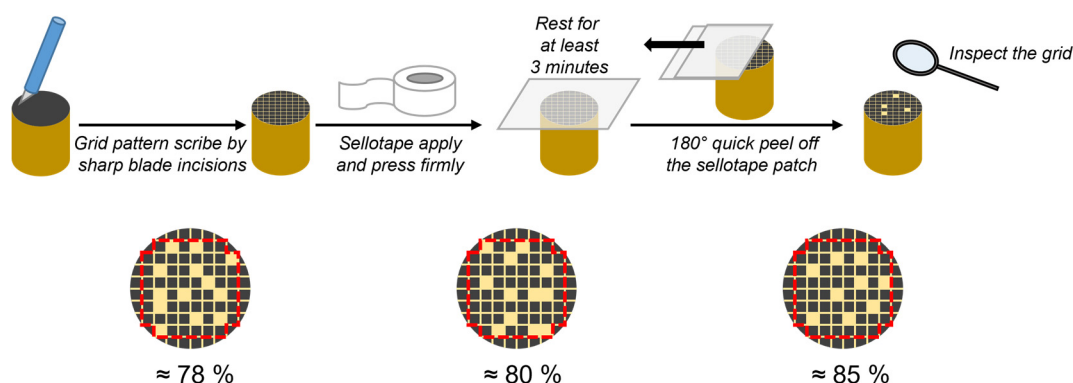
## 2. Experimental

### 2.1. Materials and Methods

In this work, a brass specimen was used as a working sample for the corrosion exploration. The chemical constitution of the brass is: Cu% 65.60, Zn% 34, Fe% 0.29, Si% 0.06, Pb% 0.05; and the corrosive solution was 0.5 M  $\text{H}_2\text{SO}_4$  that was acquired by dilution of AG 96%  $\text{H}_2\text{SO}_4$  (from Merck) with bi-distilled water. All chemicals were reagent grade, sodium 1-dodecanesulfonate (1SSD), N-methylpyrrole (NMPY), 2-methylthiophene (2 MT) were taken from Aldrich (>98%), oxalic acid dehydrate ( $\text{H}_2\text{C}_2\text{O}_4$ ) was obtained from Merck. In all determinations, the solutions for synthesis were realized by bi-distilled water: NMPY 0.1 M, 1-SSD 0.02 M, 2 MT 0.1 M, and 0.3 M  $\text{H}_2\text{C}_2\text{O}_4$ . Electrochemical polymerization and exploration of novel polymer coatings were carried out by a single-electrochemical cell of the three standard electrodes set up at room temperature. The electrochemical cell was attached to a VoltaLab potentiostat/galvanostat connected to PC operating VoltMaster software. A saturated calomel electrode (SCE) has been utilized as the reference electrode, and a platinum plate as an auxiliary electrode. The working sample is brass in cylindrical form and of a surface of  $0.5 \text{ cm}^2$ . This shape is selected because it provides an appreciable and borderless area. The working specimen was mechanically abraded by a succession of emery papers of varied dimensions (200–4000 grid) up to mirror-sheen. Then, the brass specimen was cleansed in benzene to remove all remnants of grease; after that, it was washed in bi-distilled water, dried at room temperature, and placed in the electrochemical cell. All determinations were effectuated at  $25 \text{ }^\circ\text{C}$  in atmospheric oxygen without stirring. Above the electrodeposition of the composite layers, the brass electrode was passivated in 0.3 M oxalic acid solution by cyclic voltammetry over a field potential of  $-500 \text{ mV}$  up to  $1200 \text{ mV}$  for SCE on a potential scan rate  $20 \text{ mV/s}$  by implementing 4 cycles. The poly (N-methylpyrrole–1SSD/2 methylthiophene) coatings were electrodeposited from 0.1 M N-methylpyrrole, 0.02 M 1-SSD, 0.1 M 2-methylthiophene and 0.3 M oxalic acid onto brass passivated substrate by potentiostatic and galvanostatic process (Scheme 1). Each experimental assay was repeated three times to verify the reproducibility. Electrochemical polymerization has been obtained by potentiostatic procedure at the applied potential:  $1.1 \text{ V}$ ,  $1.2 \text{ V}$ , and  $1.4 \text{ V}$  and by the galvanostatic process to constant current densities  $0.5 \text{ mA/cm}^2$ ,  $1 \text{ mA/cm}^2$ , and  $3 \text{ mA/cm}^2$  and in different molar ratios (3:5 and 5:3) and the electrodeposition was allowed for 20 and 30 min. The electrochemical comportment of coatings was considered in a solution of 0.3 M oxalic acid by cyclic voltammetry procedure. The anti-corrosion protection of the covered and uncovered samples was explored by potentiostatic and potentiodynamic polarization practices and by electrochemical impedance spectroscopy in acidic media. Additionally, long-term corrosion investigations of the coatings at various intervals up to 144 h in sulfuric acid medium by the electrochemical methods were carried out. Examination of Tafel polarization curves was performed by sweeping the potential from cathodic to anodic potentials for open circuit potential at a scan rate of  $2 \text{ mV/s}$ . Electrochemical impedance spectroscopy determinations were performed in the frequency range of  $100,000 \text{ Hz}$  to  $0.04 \text{ Hz}$ , and signal amplitude was  $10 \text{ mV}$ , to the open circuit potential of coated and uncoated specimens. All potentials have been registered versus the SCE. The adhesion of the coating was performed by the “standard sellotape test”, was achieved by the “standard sellotape test” which depicts cutting the film into small squares, sticking the tape, and then removing it. Proportional adherence has been achieved by considering the report of the number of remaining adherent cover squares to the total number of squares (see Scheme 2).



**Scheme 1.** Diagram of the electrochemical deposition procedure (Ref. = SCE reference electrode, WE = brass working sample, CE = platinum sheet counter electrode).



**Scheme 2.** Diagram for evaluation of film coating adhesion by “standard sellotape test”.

## 2.2. Instruments

A VoltaLab PGZ 402 potentiostat/galvanostat setup was employed in all electrochemical experiments. The coating was performed by Bruker optics FT-IR spectrometer by ATR attachment (with a diamond crystal) in the spectral range  $4000\text{--}650\text{ cm}^{-1}$  at a resolution of  $4\text{ cm}^{-1}$ .

Morphologies of coated samples were considered by scanning electron microscope (SEM). Specimen morphology analysis was accomplished by SEM in a dual beam FEI Quanta 3D FEG model, working in a high vacuum means with an accelerating voltage of 15 to 30 kV. Minimal specimen preparation involves immobilizing the electrodes on a double-sided carbon tape without coating.

## 3. Results and Discussion

### 3.1. Electrochemical Synthesis of PNMPY-1-SSD/P2MT Coating on Brass

The electropolymerization of NMPY-1SSD and 2MTP monomers was carried out by employing the potentiostatic and galvanostatic procedures on the surfaces of the passivated brass substrate. The passivation method has been realized by utilizing the voltammetry

practice in the domain from  $-0.5$  V to  $1.4$  V vs. SCE at a  $20$  mV/s scan rate in  $0.3$  M oxalic acid solution by applying four cycles, and this process was presented in previous papers [27,32–34]. The insoluble compounds attained by the passivation mechanism are copper oxides and copper oxalates, which impede the dissolution of the metal without hindering the electropolymerization procedure. The passivated specimen brass under the electropolymerization process has also been introduced in the specialty literature [28–34]. By improving the polymerization features, we can obtain polymeric films of PNMPY-1SSD/P2MT that have a meaningful corrosion protection effect. The electropolymerization of NMP and 2 MT monomers was performed onto passivated brass substrates. Following passivation, the electropolymerization of the monomers was established without changing the polymerization circumstances. A valuable deposition requires obtaining a passive film, which could be effective in preventing the dissolution of the oxidizable metal without obstructing the permissiveness of the monomer and its subsequent oxidation. The final result is to acquire a homogenous polymeric layer, compact and adhering to the sample surface. The PNMPY-1SSD/P2MT composite coating has been accomplished from  $0.3$  M oxalic acid,  $0.1$  M N-methylpyrrole,  $0.02$  M sodium 1-dodecanesulfonate, and  $0.1$  M 2-methylthiophene by potentiostatic practice at:  $1.1$  V,  $1.2$  V and  $1.4$  V applied potential and by galvanostatic proceeding at current densities:  $0.5$  mA/cm<sup>2</sup>,  $1$  mA/cm<sup>2</sup> and  $3$  mA/cm<sup>2</sup> in varied molar ratio. The electrodeposition was allowed for  $20$  min and  $30$  min. From Figure 1, it can be noted that “current density–time” curves achieved during the constitution of PNMPY-1SSD/P2MT coatings on brass at  $1.1$  V,  $1.2$ , and  $1.4$  V applied potential in various molar ratios. Following the oxidation time of  $1200$  s and  $1800$  s, the initial format of the “current density–time” curves during the evaluation of the polymer electrodeposition shows that this depositing has been determined by nucleation and growth onto the brass substrate [12,20–24].

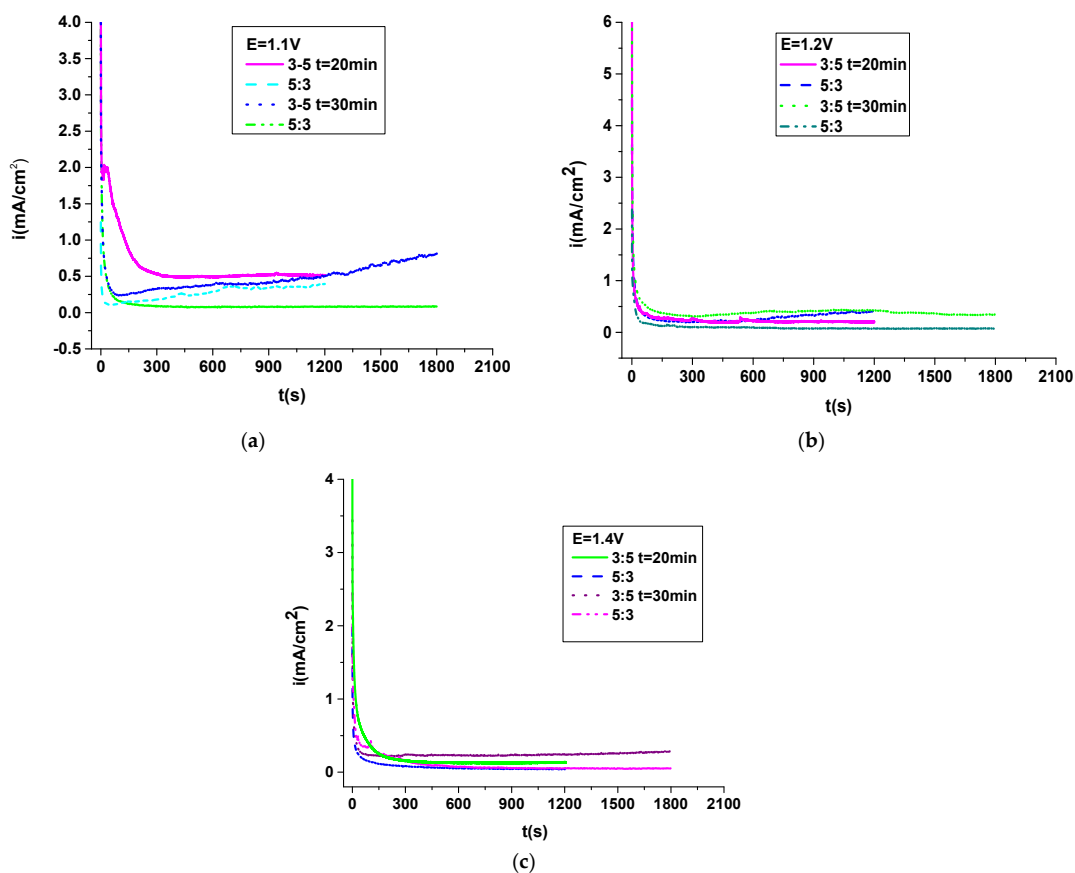


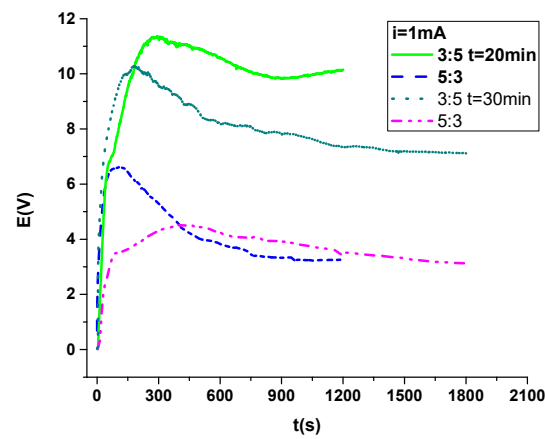
**Figure 1.** Potentiostatic electrodepositions of PNMPY-1SSD/P2MT/brass to potential (a)  $E = 1.1$  V, (b)  $E = 1.2$  V and (c)  $E = 1.4$  V vs. SCE for  $1200$ – $1800$  s in varied molar ratio for PNMPY-1SSD and P2MT.

At first, the current suddenly decreased owed to the electro-adsorption of the electrolyte and PY-MT monomers. Subsequent to about 40 s, the current raised, and this is owing to the dissolving of the passive layer and forming of the polymer on the brass surface. In the last step, the current was kept constant as the composite films were achieved on the brass electrode. The transient change of the upper part is linear with the variation of the nucleation time, the electrochemical verification, and the differentiation in the molar ratio of PPY: NEA. At the time when the applied potential was 1.1 V at 5:3 and 3:5 molar ratio, the current was almost constant at 0.6 mA/cm<sup>2</sup> and 0.8 mA/cm<sup>2</sup>, the current was higher than in other situations of potentiostatic deposition, and the acquired coatings were uniform and adherent. Additionally, it can be observed in Figure 1 that the potentiostatic deposition at 1.1 V applied constant potential in 3:5 for NMPY: 2 MT molar ratio has a greater induction time for attained of PMPY-1SSD/2MT coating, and it was of less advantageous to the formation of a polymeric film of superior characteristics. Electrochemical features such as the applied potential were instituted to have a large effect on the induction time. It should be noted that the 1.4 V, 1.2 V, and 1.1 V applied constant potential in 5:3 and 3:5 molar ratio for PPY: PNEA has a little induction time for the development of the deposited layer, and it was favorable for obtaining the coating's superior quality. The anionic surfactant 1SSD similar to a dopant ion utilized in electrodeposition (introduced in methylpyrrole), can have an important impact on the selectivity of ion enhancement by assuring the conductivity of the polymer. The visual investigation of the brass sample following electrochemical polymerization indicates the constitution of a black PNMPY-1SSD/P2MT layer. The coating is dense, homogeneous, and adherent to the brass electrode. Adhesion of the coating, as evaluated by "the standard sellotape", was established to be ~85% [30–33].

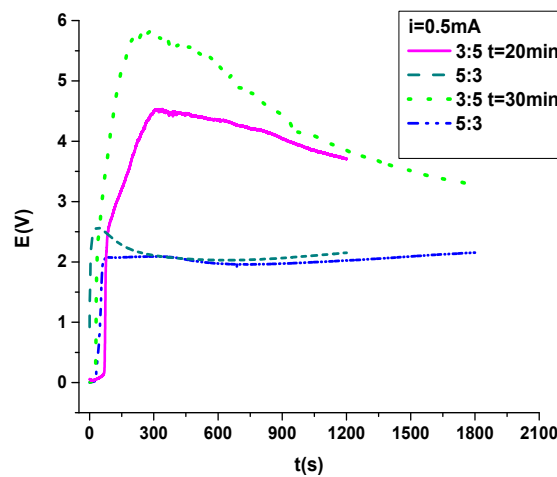
Figure 2 shows the "potential-times" curves acquired by obtaining the polymeric layer as poly (N-methylpyrrole-sodium 1-dodecanesulfonate/2-methylthiophene) on the brass substrate (PNMPY-1SSD/P2MT/brass) at varied applied current densities in various molar ratio. Following the oxidation interval of 1200 s and 1800 s, the initial form of the "potential-time" curves by the polymer electrochemical deposition practice designates that the electrodeposition was realized by "nucleation and growth" onto brass substrate [12,16–21]. Examining Figure 2, at applied current densities of 0.5 mA/cm<sup>2</sup> and 1 mA/cm<sup>2</sup> at some molar ratios, lower induction range results, and induction interval as less than 10 s was noted in the electrochemical polymerization of the layer composite of NMPY-1SSD and 2 MT and its value decreases by rising the molar ratio and the raising of the nucleation potential. The polymerization potential is different between 6 V and 11 V versus SCE for applied current densities: 0.5 mA/cm<sup>2</sup> and 1 mA/cm<sup>2</sup> in 5:3 and 3:5 molar ratios for NMPY-1SSD and 2 MT. The coatings possess the densest and most adherent appearance at applied current densities of about 0.5 mA/cm<sup>2</sup>. The visual verification of the brass sample surface following deposition divulges the constitution of a black-colored PNMPY-1SSD/P2MT/brass layer. The adhesion of the coating assessed by "the standard sellotape" was determined to be ~78%–80%.

### 3.2. Electrochemical Characterization PNMPY-1SSD/P2MT Coating

The electrochemical comportment of the modified PNMPY-1SSD/P2MT/brass electrode in a monomer-free 0.3 M oxalic acid is shown in Figure 3 to the potential range of –0.3 and +1.2 V vs. SCE and the scan rate of 20 mV/s. Cyclic voltammetry practice was effectuated in the extended potential interval in order to examine all the physical and electrochemical characteristics of this composite. Analyzing Figure 3, it can be said that the electrochemical behavior of coating is affected by the number of cycles and the electrochemical deposition characteristics. The endurance of any conducting polymer in reduced and oxidized conditions is a relevant feature for various applications. The essential cause that constitutes the lifetime of a conducting polymer is the constant chemical attendance of the matrix itself [4,27–31]. The steadfastness PNMPY-1SSD/P2MT composite was established by cyclic voltammetry in a monomer-free oxalic acid solution (see Figure 3).

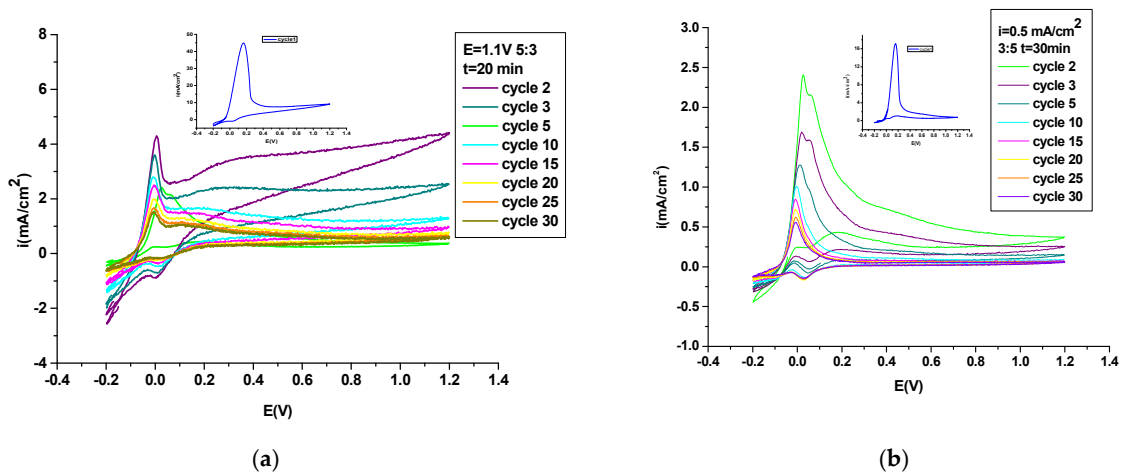


(a)



(b)

**Figure 2.** Galvanostatic electrodepositions of PNMPY-1SSD/P2MT/brass (a) at  $i = 1 \text{ mA/cm}^2$  and (b)  $i = 0.5 \text{ mA/cm}^2$  current densities for 1200–1800 s in varied molar ratio for PNMPY-1SSD and P2MT.



(a)

(b)

**Figure 3.** Cyclic voltammograms of PNMPY-1SSD/P2MT/brass coating obtaining at (a)  $E = 1.1 \text{ V}$  and (b) at  $i = 0.5 \text{ mA/cm}^2$ , in  $0.3 \text{ M H}_2\text{C}_2\text{O}_4$  solution monomer free at potential interval  $-0.3$  and  $1.2 \text{ V}$  vs. SCE a and scan rate of  $20 \text{ mV/s}$ .

Thus, this composite could often be cycled from the oxidized and reduced form without considerable degradation of the polymeric composite; the current density diminishes by each cycle and eventually reaches a constant value. The polymer that shows a minimum decrease in current density at repetitive cycling (except the first cycle, which is more intense) is electrochemically more stable.

### 3.3. FT-IR Examination

The new composite coatings were explored by FT-IR spectroscopy (see Figure 4) in the spectral range  $4000\text{--}650\text{ cm}^{-1}$  at a resolution of  $4\text{ cm}^{-1}$  (over five scans). FT-IR procedures can be employed to highlight the type of binding used to acquire a new polymeric composite. Representative peaks in the transmittance spectrum of PNMPY-1SSD/P2MT/brass coverings are shown in Figure 4. The FT-IR outcomes describe the appearance of the considerable absorption bands noticed in PNMPY and P2MT deposited onto the brass substrate.

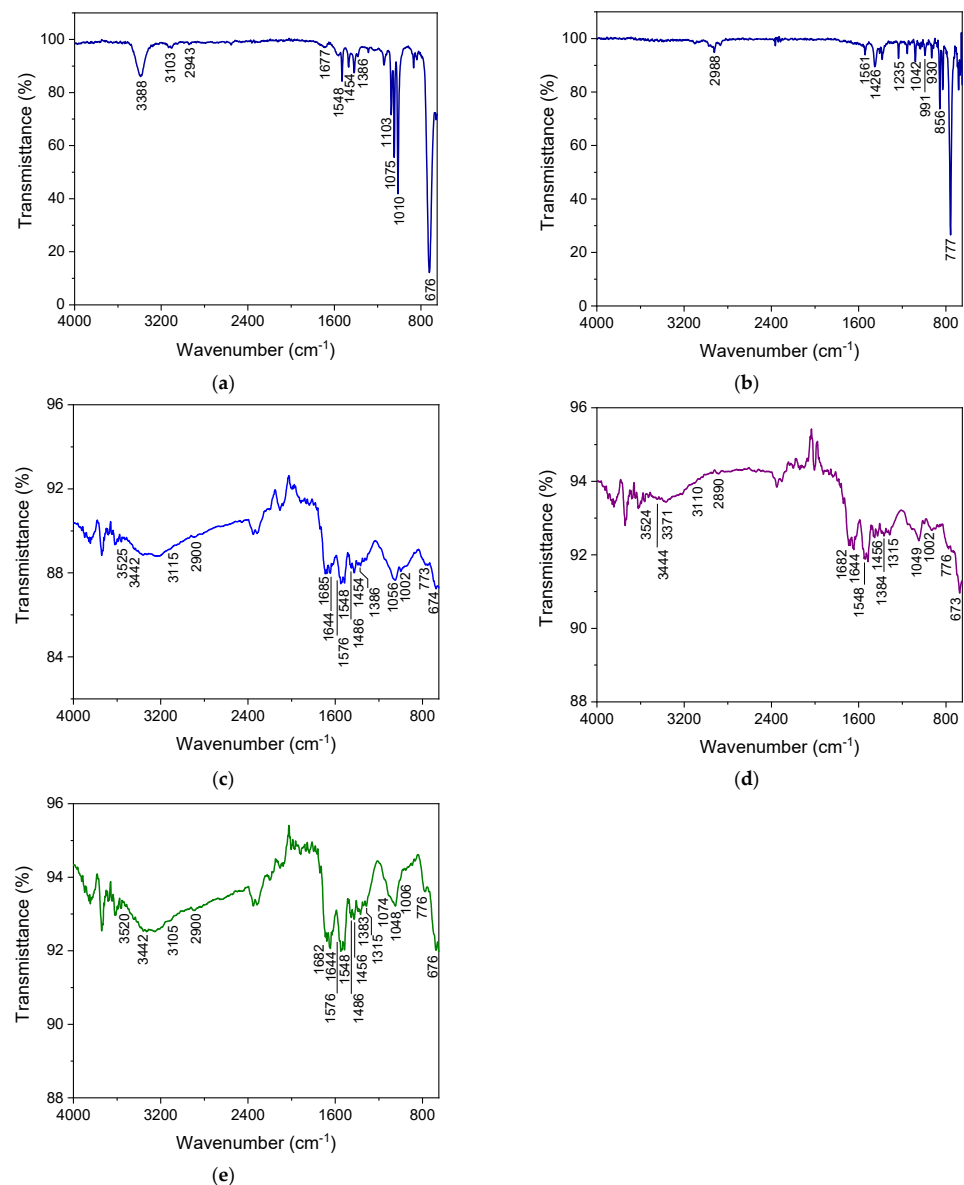


**Figure 4.** The FT-IR spectra of (a) NMPY), (b) 2 MT, and (c–e) PNMPY-1SSD/P2MT/brass deposition on the brass sample at galvanostatic and potentiostatic method (c)  $0.5\text{ mA/cm}^2$ , (d)  $1.2\text{ V}$  and (e)  $1.4\text{ V}$  in 5:3 molar ratio for MPY-1SSD: 2 MT.

The important peaks in the transmittance spectrum of NMPY (monomer) and 2 MT (monomer) that were exposed in Figure 4a,b are the outcome of the spectrum of NMPY, shown in Figure 4a, where the significant features of bands for the aromatic ring in NMPY are obvious to 1548 and 1454  $\text{cm}^{-1}$  for C=C stretching, being clearly noted. The band positioned at 1677 and 1634  $\text{cm}^{-1}$  is related to the C=C stretching. The characteristic bands at 1386 and 1315  $\text{cm}^{-1}$  are attributed to the N-H stretching vibration of the pyrrole ring. The small peak at 2943  $\text{cm}^{-1}$  is ascribed to the  $\text{CH}_3$  stretch of the N-methylpyrrole units. Peaks that can be assigned as “in-plane and out-of-plane” of the CH chains at 1103, 1075, and 676  $\text{cm}^{-1}$  are noted in the polymer. From Figure 4b, the spectrum of 2 MT shows the peak at 2988  $\text{cm}^{-1}$  is designated to the  $\text{CH}_3$  stretch of 2-methylthiophene parts, and the peaks corresponding to the asymmetric and symmetric C=C stretching vibrations of the 2 MT ring are observed at 1561  $\text{cm}^{-1}$  and 1426  $\text{cm}^{-1}$ . The band appearing at about 1042  $\text{cm}^{-1}$  and 777  $\text{cm}^{-1}$  shows the C-S-C stretching vibration of the thiophene ring. The spectra of PMPY-1SSD/P3MT/brass electrochemical deposition by potentiostatic and galvanostatic procedures are displayed in Figure 4c–e. The bands observed at 3472 and 3106  $\text{cm}^{-1}$  are assigned to the N-H stretching vibration in the polymer. The peaks showing at about 3520 and 3442  $\text{cm}^{-1}$  correspond to the OH stretch of the counterions. The band about 3100–2900  $\text{cm}^{-1}$  is attributed to the  $\text{CH}_3$  stretching of N-methylpyrrole components. The peak at about 1226  $\text{cm}^{-1}$  describes the C-N of the pyrrole ring. Significant assignments of the aromatic ring peaks in PNMPY are apparent at 1576, and 1456  $\text{cm}^{-1}$  for C=C stretch, being obviously decided. The appearance absorption bands located at 1574, 1548, 1486, and 1456  $\text{cm}^{-1}$  are disclosed in the stretching vibration of the quinoid rings (Figure 4c–e). The peaks positioned at 1386 and 1315  $\text{cm}^{-1}$  are attached to N-H stretching vibration of the methylpyrrole ring; the bands at 1664 and 1644  $\text{cm}^{-1}$  are associated with the C=C stretching. In the composite coverage spectrum, bands corresponding to the asymmetric and symmetric C=C stretching vibrations of the 2-methylthiophene ring are noted at 1568  $\text{cm}^{-1}$  and 1456  $\text{cm}^{-1}$  (Figure 4c–e) [19,31–36]. The bands disclosed around 1049  $\text{cm}^{-1}$  and 773  $\text{cm}^{-1}$  submit the C-S-C stretching vibration of the 2-methylthiophene ring, and the band at about 1536  $\text{cm}^{-1}$  is related to the C=C stretching vibration. The bands placed at 1454 and 1315  $\text{cm}^{-1}$  are connected to the “stretching vibration” of the  $\text{CH}_2$  and  $\text{CH}_3$  constituents in the anionic surfactant, and the small peaks around 1074  $\text{cm}^{-1}$  and 673  $\text{cm}^{-1}$  are ascribed to the S=O stretching vibration of surfactant anion. The appearance of the bonds C=O and CH are shown by stretching modes at 1682  $\text{cm}^{-1}$  and 1248  $\text{cm}^{-1}$ , which were most likely linked to the consolidation of the surfactant in the polymer matrix (see Figure 4c–e). Peaks at about 1075, 831, 776, and 1006  $\text{cm}^{-1}$  are assigned to the “in-plane” and “out-of-plane” C-H of the aromatic rings and to the “out-of-plane” vibration of C-H doped of PNMPY in oxalic acid solution (Figure 4c–e). [19,36–38]. The bands at approximately 711  $\text{cm}^{-1}$  and 674  $\text{cm}^{-1}$  may ensue from the O=C=O and C-C-O in-plane deformation of the oxalate anion. Distinguishing “in-plane” and “out-of-plane” of the N-H bond peaks at 1049, 1141, and 673  $\text{cm}^{-1}$  are presumed to be adequate in the PNMP-1SSD/P2MT/brass composite coating. Comparing Figure 4a,b by Figure 4c,e, it can be supposed that the PNMPY-1SSD/P2MT composite is electrochemically deposited onto the brass substrate. The peaks related to the monomer spectrum (MPY and 2 MT) are shown in the spectrum of the composite coating (PNMPY-1SSD/P2MT) on the brass substrate.

### 3.4. Electrochemical Analysis

#### 3.4.1. Potentiodynamic Polarization Practice

The anti-corrosive characteristics of the acquired PNMPY-1SSD/P2MT/brass composite were explored in 0.5 M  $\text{H}_2\text{SO}_4$  by potentiodynamic polarization process and electrochemical impedance spectroscopy. The polarization curves of bare and coated PNMPY-1SSD/P2MT brass in 0.5 M  $\text{H}_2\text{SO}_4$  media are shown in Figures 5–7. Additionally, the polarization behavior of the brass sample was considered by brass-coated PNMPY-1SSD/P2MT composite performed by potentiostatic and galvanostatic procedures at varying current

densities in various quantities and different deposition periods. In this research, one of the greatest procedures for the protection activity of brass in corrosive media is the application of composite coatings, which investigate the corrosion of anodic or cathodic mechanism and both. The surfaces coated with the PNMPY-1SSD/P2MT composite explicated considerable attenuation of the anodic and cathodic currents, which indicated the diminution of the cathodic and anodic mechanisms.

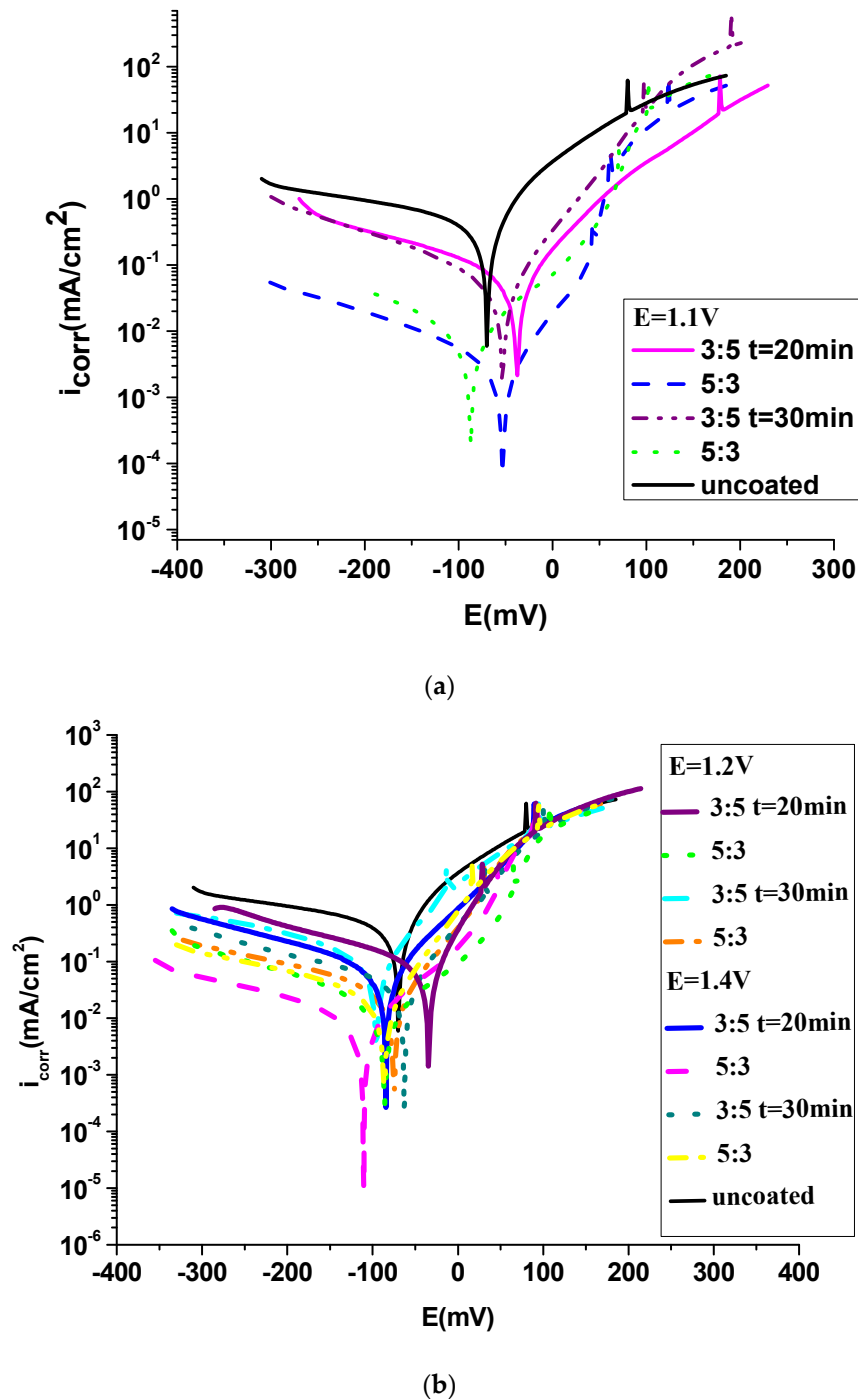


**Figure 5.** Polarization curves of PNMPY-1SSD/P2MT coated and uncoated over the brass substrate in 0.5 M H<sub>2</sub>SO<sub>4</sub> by potentiostatic practice at (a) 1.1 V and (b) 1.2 V and 1.4 V potential applied at varied molar ratios and the electrochemical deposition was allowed for 20 and 30 min.

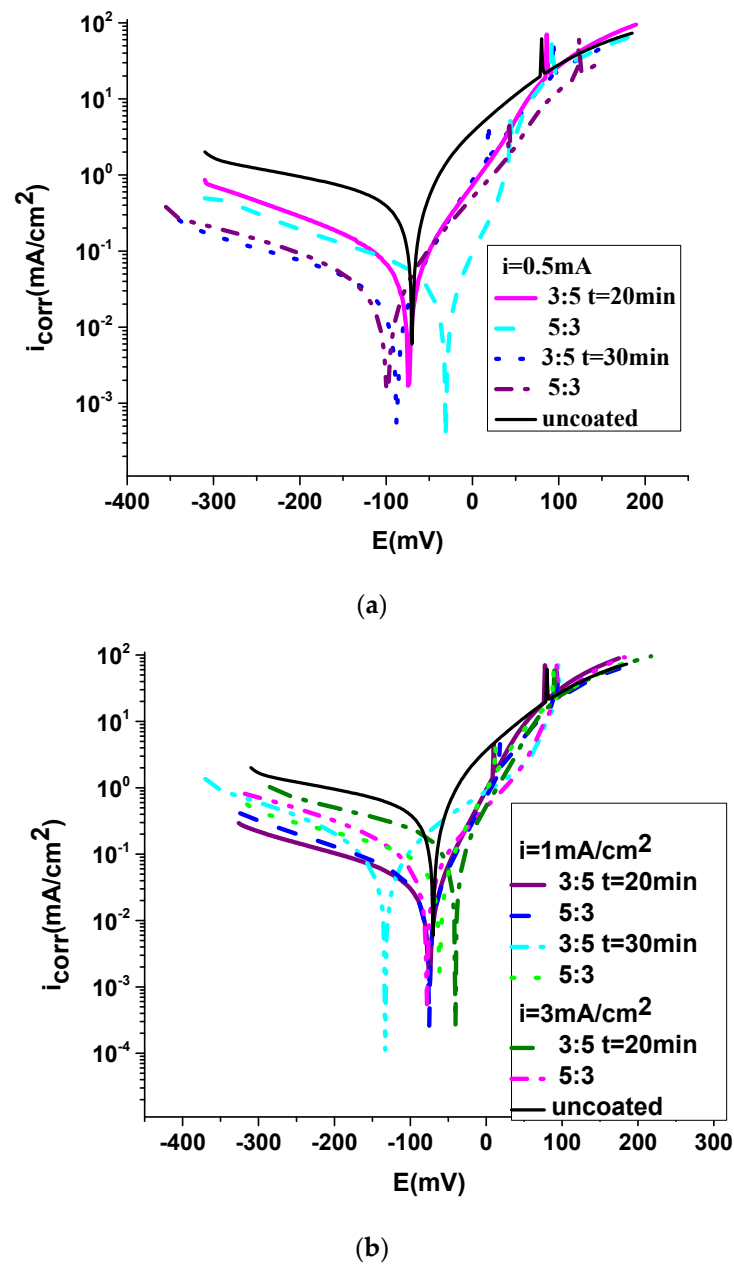
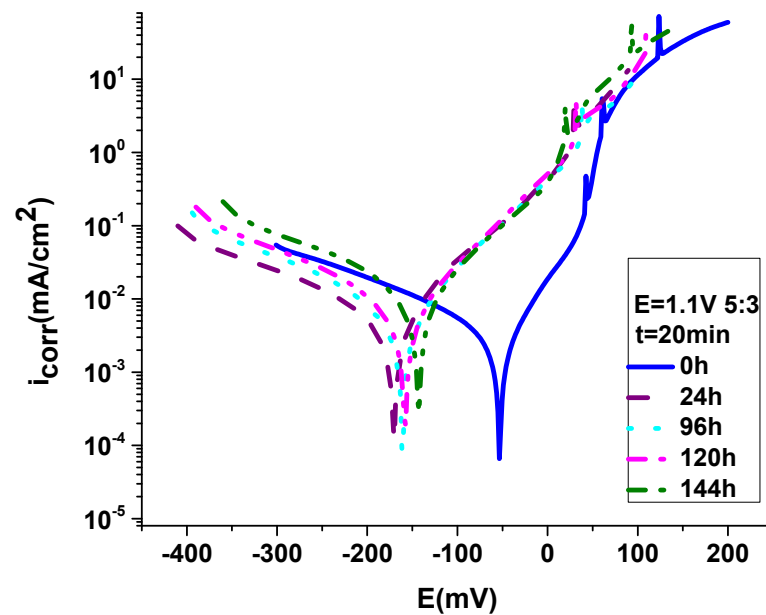


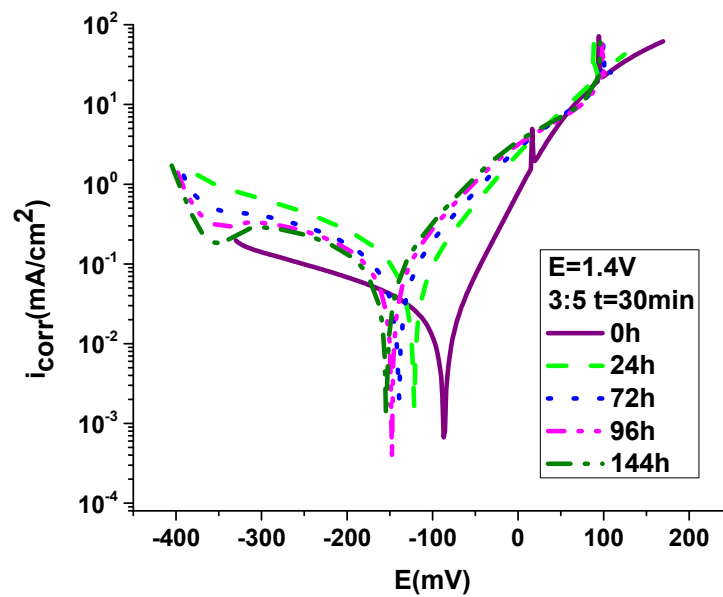
**Figure 6.** Polarization curves of PNMPY-1SSD/P2MT covered and uncovered onto the brass substrate in 0.5 M sulfuric acid by galvanostatic procedure at (a) 0.5 mA/cm<sup>2</sup> and (b) 1 mA/cm<sup>2</sup> and 3 mA/cm<sup>2</sup> current density in several molar ratios and the electrochemical polymerization was permissive for 20 and 30 min.

Additionally, electrochemical determinations were carried out effectuated in 0.5 M H<sub>2</sub>SO<sub>4</sub> solution to evaluate the protective activity of the organic layers against corrosion. It can be seen from Figures 5–7 that both the anodic metal dissolving and cathodic hydrogen reduction reactions have been prevented by the electrochemical deposition of these PNMPY-1SSD/P2MT coatings in the aggressive medium. This case disclosed that this covering had significant results of cathodic and anodic reactions of the electrochemical procedure. The corrosion potential ( $E_{\text{corr}}$ ), corrosion current density ( $i_{\text{corr}}$ ), anodic and cathodic Tafel slopes were determined by extrapolating the linear parts of the anodic and cathodic Tafel branches of brass electrode covered by PNMPY-1SSD/P2MT composite are submitted in Tables 1–3. By exploring these polarization curves, it can be noted that the corrosion potential of the coated brass substrate is shifted to a more positive potential compared to the bare specimen.

This event can be due to the attack of corrosive compounds that reach the pores of the layer as a result of the formation of passive films that impede the corrosion of brass samples.



(a)



(b)

**Figure 7.** Polarization curves PNMPY-1SSD/P2MT of uncoated and coated brass specimens in sulfuric acid solution by electrochemical polymerization at (a)  $E = 1.1\text{ V}$  and (b) at  $E = 1.4\text{ V}$  in various molar ratios at differing immersion times.

**Table 1.** Kinetic corrosion parameters of uncoated and coated brass sample in 0.5 M sulfuric acid solutions at 25 °C.

The System PNMPY-1SSD/P2MT/Brass	$E_{corr}$ (mV)	$i_{corr}$ (mA/cm <sup>2</sup> )	$R_p$ ( $\Omega$ cm)	$R_{mpy}$	$P_{mm/year}$	$K_g$ (g/m <sup>2</sup> h)	$b_a$ (mV/decade)	$-b_c$ (mV/decade)	E (%)	%P
Brass + 0.5 M H <sub>2</sub> SO <sub>4</sub>	-73	0.185	55	84.88	2.15	2.09	78	130	-	-
PNMPY-1SSD/P2MT 1.1 V 3:5 molar ratio, t = 20 min	-56	0.030	399	13.76	0.35	0.34	56	126	81	0.078
PNMPY-1SSD/P2MT 1.1 V 5:3 molar ratio, t = 20 min	-55	0.002	6310	0.93	0.023	0.022	62	117	98	0.006
PNMPY-1SSD/P2MT 1.1 V 3:5 molar ratio, t = 30 min	-56	0.027	439	12.85	0.33	0.32	53	114	85	0.072
PNMPY-1SSD/P2MT 1.1 V 5:3 molar ratio, t = 30 min	-99	0.006	2520	2.75	0.07	0.06	73	113	96	0.008
PNMPY-1SSD/P2MT 1.2 V 3:5 molar ratio, t = 20 min	-86	0.034	369	19.2	0.46	0.47	62	121	81	0.084
PNMPY-1SSD/P2MT 1.2 V 5:3 molar ratio, t = 20 min	-49	0.028	393	12.84	0.32	0.31	51	102	85	0.06
PNMPY-1SSD/P2MT 1.2 V 3:5 molar ratio, t = 30 min	-75	0.015	818	6.88	0.17	0.16	54	119	92	0.053
PNMPY-1SSD/P2MT 1.2 V 5:3 molar ratio, t = 30 min	-90	0.013	983	5.96	0.15	0.14	52	120	93	0.037
PNMPY-1SSD/P2MT 1.4 V 3:5 molar ratio, t = 20 min	-86	0.033	359	19.2	0.46	0.47	62	123	81	0.091
PNMPY-1SSD/P2MT 1.4 V 5:3 molar ratio, t = 20 min	-111	0.006	2890	2.75	0.07	0.06	68	125	96	0.005
PNMPY-1SSD/P2MT 1.4 V 3:5 molar ratio, t = 30 min	-63	0.020	509	9.17	0.23	0.22	53	139	89	0.074
PNMPY-1SSD/P2MT 1.4 V 5:3 molar ratio, t = 30 min	-90	0.011	982	5.04	0.13	0.12	51	120	94	0.05

**Table 2.** Kinetic corrosion parameters of uncoated and coated brass sample in 0.5 M sulfuric acid solutions at 25 °C.

The System PNMPY-1SSD/P2MT/Brass	$E_{corr}$ (mV)	$i_{corr}$ (mA/cm <sup>2</sup> )	$R_p$ ( $\Omega$ cm)	$R_{mpy}$	$P_{mm/year}$	$K_g$ (g/m <sup>2</sup> h)	$b_a$ (mV/decade)	$-b_c$ (mV/decade)	E (%)	%P
Brass + 0.5 M H <sub>2</sub> SO <sub>4</sub>	-73	0.185	55	84.88	2.15	2.09	78	130	-	-
PNMPY-1SSD/P2MT 1 mA/cm <sup>2</sup> 3:5 molar ratio, t = 20 min	-78	0.019	636	8.71	0.22	0.214	46	129	90	0.071
PNMPY-1SSD/P2MT 1 mA/cm <sup>2</sup> 5:3 molar ratio, t = 20 min	-78	0.017	647	7.8	0.19	0.18	46	99	91	0.068
PNMPY-1SSD/P2MT 1 mA/cm <sup>2</sup> 3:5 molar ratio, t = 30 min	-130	0.037	319	18.8	0.47	0.46	82	98	80	0.03
PNMPY-1SSD/P2MT 1 mA/cm <sup>2</sup> 5:3 molar ratio, t = 30 min	-98	0.034	350	17.8	0.45	0.43	49	130	82	0.062
PNMPY-1SSD/P2MT 0.5 mA/cm <sup>2</sup> 3:5 molar ratio, t = 20 min	-81	0.025	359	11.5	0.30	0.28	60	125	87	0.078
PNMPY-1SSD/P2MT 0.5 mA/cm <sup>2</sup> 5:3 molar ratio, t = 20 min	-51	0.018	543	8.25	0.21	0.20	48	87	90	0.052
PNMPY-1SSD/P2MT 0.5 mA/cm <sup>2</sup> 3:5 molar ratio, t = 30 min	-90	0.015	846	6.88	0.17	0.16	50	122	92	0.031
PNMPY-1SSD/P2MT 0.5 mA/cm <sup>2</sup> 5:3 molar ratio, t = 30 min	-100	0.013	878	5.96	0.15	0.14	62	114	93	0.026
PNMPY-1SSD/P2MT 3 mA/cm <sup>2</sup> 3:5 molar ratio, t = 20 min	-79	0.038	331	17.43	0.44	0.43	71	111	80	0.088
PNMPY-1SSD/P2MT 3 mA/cm <sup>2</sup> 5:3 molar ratio, t = 20 min	-49	0.037	351	16.97	0.43	0.42	57	121	80	0.053

Exploration of the polarization curves from Figures 5 and 6 and Tables 1–3 revealed that the electrochemical parameters of bare and coated brass sample by deposition at 1.1 V, 1.2 and 1.4 V potential applied and 0.5 mA/cm<sup>2</sup>, 1 mA/cm<sup>2</sup>, and 3 mA/cm<sup>2</sup> current density

and at 20 min and 30 min for 5:3 and 3:5 molar ratio of PNMPY-1SSD/P2MT were lower than those for brass in 0.5 M H<sub>2</sub>SO<sub>4</sub> solution. The greatest protective effect was performed at 1.1 V and 1.4 V potential and 0.5 mA/cm<sup>2</sup> and 1 mA/cm<sup>2</sup> current density to 5:3 molar ratio of PNMPY-1SSD/P2MT. This coating composition has a superior protective capacity that the polymer PNMPY layer has been doped with an anionic surfactant of sodium 1-dodecanesulfonate. This sodium 1-dodecanesulfonate surfactant as a dopant ion used in electrodeposition (existing in N-methylpyrrole) can have a considerable result by the ion modifying the selectivity by providing the conductivity of the polymer. The attendance of the hydrocarbonate chains of the anionic surfactant that “competitively adsorb” on the brass electrode prevents the acting centers, and as a result, the SO<sub>4</sub><sup>2-</sup> aggressive element is hindered from attacking the brass surface and protecting action is performed [33–38].

**Table 3.** Kinetic corrosion parameters of uncoated and coated brass sample in 0.5 M sulfuric acid solutions at 25 °C at different immersion times.

The System PNMPY-1SSD/P2MT/Brass	E <sub>corr</sub> (mV)	i <sub>corr</sub> (mA/cm <sup>2</sup> )	R <sub>p</sub> (Ωcm)	R <sub>mpy</sub>	P <sub>mm/year</sub>	K <sub>g</sub> (g/m <sup>2</sup> h)	b <sub>a</sub> (mV/ decade)	−b <sub>c</sub> (mV/ decade)	E (%)
Brass + 0.5 M H <sub>2</sub> SO <sub>4</sub>	−73	0.185	55	84.88	2.15	2.09	78	130	-
PNMPY-1SSD/P2MT 1.1 V 3:5 molar ratio, t = 20 min 0 h	−55	0.002	6310	0.93	0.023	0.022	62	117	98
PNMPY-1SSD/P2MT 1.1 V 3:5 molar ratio, t = 20 min 24 h	−161	0.0028	5020	1.28	0.032	0.031	62	111	98
PNMPY-1SSD/P2MT 1.1 V 3:5 molar ratio, t = 20 min 72 h	−164	0.0031	4434	1.42	0.036	0.035	64	96	98
PNMPY-1SSD/P2MT 1.1 V 3:5 molar ratio, t = 20 min 96 h	−160	0.0038	3600	1.74	0.044	0.043	66	99	98
PNMPY-1SSD/P2MT 1.1 V 3:5 molar ratio, t = 20 min 144 h	−144	0.005	2333	2.29	0.058	0.056	68	94	97
PNMPY-1SSD/P2MT 1.4 V 5:3 molar ratio, t = 30 min 0 h	−90	0.011	982	5.04	0.13	0.12	61	120	94
PNMPY-1SSD/P2MT 1.4 V 5:3 molar ratio, t = 30 min 48 h	−123	0.036	396	16.5	0.42	0.41	66	969	81
PNMPY-1SSD/P2MT 1.4 V 5:3 molar ratio, t = 30 min 72 h	−132	0.040	366	18.35	0.45	0.44	71	112	80
PNMPY-1SSD/P2MT 1.4 V 5:3 molar ratio, t = 30 min 96 h	−139	0.041	362	18.81	0.47	0.46	69	121	78
PNMPY-1SSD/P2MT 1.4 V 5:3 molar ratio, t = 30 min 144 h	−141	0.043	375	19.79	0.5	0.49	69	122	77

The experimental results show that the corrosion rate of PNMPY-1SSD/P2MT covered brass was approximately ~9 times lower than that remarked for uncoated brass. It is clear that these coatings stopped the offense of the aggressive factor (H<sub>2</sub>SO<sub>4</sub>) on the brass specimen. The corrosion behavior of PNMPY-1SSD/P2MT coating established that the covered brass had remarkably greater anti-corrosion performance and lower corrosion rate than the uncovered brass sample.

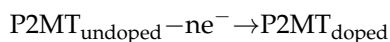
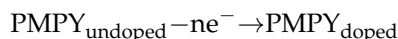
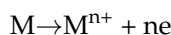
The result of raising the 0–144 h immersion interval on corrosion protection of PNMPY-1SSD/P2MT coatings to brass corrosion in 0.5 M sulfuric acid has been explored by potentiodynamic polarization (polarization curves). The impact of protection effectiveness of these composites by immersion times is displayed in Figure 7 and Table 3. It can be noted from Figure 7 and Table 3 that the protection efficiency slowly diminishes with growth in time. It can be seen that during the continuation of the immersion period, the corrosion rate of the coating layer obtained at 1.1 V (3:5 molar ratio, t = 20 min) remains constant, but for composites achieved at 1.4 V (5:3 molar ratio, t = 20 min) from 96 h, a slight increase in corrosion rate and decrease in protection yield. This result is due to the deterioration of the surface morphology by raising immersion time as a result of the modification of the active surface and can be established to the accompanying defects of the composite film that allow the penetration of the aggressive ions into the brass/coating interface. It is also clear that after an immersion period of 96 h, the coating performance is still 97% and

80% for PNMPY-1SSD/P2MT composite acquired at 1.1 V, 3:5, t = 20 min and at 1.4 V, 5:3, t = 30 min showing that this composite is an effective long-term protector on brass in 0.5M H<sub>2</sub>SO<sub>4</sub> solution. It displayed a non-destructiveness topography after 96 h of immersion in the corrosive environment, further examining its higher protective capability. Anyway, some existing imperfections in the coating could influence the corrosion behavior over a long time of immersion in this corrosive environment. In Figures 5–7 and Tables 1–3, it is shown that the little corrosion rate and the highest anti-corrosion effect were accomplished by PNMPY-1SSD/P2MT coating at 1.1 V and 1.4 V (at 5:3 molar ratio, t = 20 and 30 min), at 0.5 mA/cm<sup>2</sup> (at 5:3 and 3:5 molar ratios, t = 30 min) applied current density (at 5:1, 3:5 molar ratio) and very good protection obtained at 1.2 V (at 5:3 molar ratio, t = 30 min) and 1 mA/cm<sup>2</sup> (at 5:3 molar ratio, t = 20 min) against to bare brass in corrosive medium-0.5 M H<sub>2</sub>SO<sub>4</sub>.

The corrosion mechanism of bare and composite-coated brass in sulfuric acid solution can be realized as follows [24–28,30–36]:

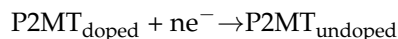
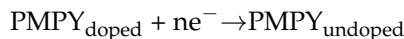
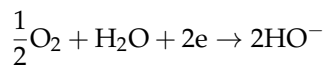
Anodic process:

-dissolution of Metal (M = Cu-Zn) as anodic process



Cathodic process:

The oxygen reduction as a cathodic reaction:



In the acidic solutions, the metal is oxidized to a higher valence estate by dissolution in an anodic reaction. Compounds dissolved in the solution as oxygen, hydrogen ions are reduced by electrons accepted from the metal in a cathodic reaction.

The porosity (P) of the coating layer (PNMPY-1SSD/P2MT) (see Tables 1 and 2) is a specific characteristic for determining when a coating layer is appropriate or not for protecting the substrate against corrosion. The porosity of the coatings has been evaluated by the subsequent relationship (1) [30–36]:

$$P = \frac{Rp(\text{uncoated})}{Rp(\text{coated})} 10^{-\frac{I\Delta E_{corr}}{\beta_a}} \tag{1}$$

P is total porosity, Rp- is the polarization resistance for bare brass and coated samples, ΔE<sub>corr</sub>-the difference from the corrosion potential of coated and uncoated electrodes, and β<sub>a</sub> is the anodic Tafel slope for brass samples. Additionally, the porosity of PNMPY-1SSD/P2MT coated brass specimen by potentiostatic and galvanostatic electrochemical deposition practice are 0.005, 0.006, 0.008, 0.026, 0.029, and 0.031 (at 1.1 V and 1.4 V potential applied and at 0.5 mA/cm<sup>2</sup> and 1 mA/cm<sup>2</sup> current densities applied in 5:3 molar ratio). The considerable size of the porosity in the PNMPY-1SSD/P2MT layers establishes an appreciable improvement of the protection result by stopping the access of the corrosive factor (SO<sub>4</sub><sup>2-</sup>) to the electrode surface and additionally diminishes the corrosion of the underlying specimen substrate. The greatest efficiency is achieved of PNMPY-1SSD/P2MT made by electrochemical deposition at an applied potential 1.1 V and 1.4 V and to a current density 0.5 mA/cm<sup>2</sup> in molar ratio 5:3. The experimental measurements obtained in

this exploration can be introduced by the protective performance of composite layer on the electrochemical ascribes of brass the specimen. It was determined that the PNMPY-1SSD/P2MT coatings indicate a lower value of porosity, denoting the showed density of the composite layer and the homogeneous constitution of the coatings.

### 3.4.2. Electrochemical Impedance Spectroscopy (EIS) Investigations

The protective action of novel PNMPY-SSD/P2MT composite coated on brass in an acidic environment was explored by electrochemical impedance spectroscopy (EIS). Impedance determinations were performed at open circuit potential in the frequency domain from 100,000 Hz to 0.04 Hz with an AC wave of  $\pm 10$  mV (peak-to-peak), and the impedance experiments were performed at a rate of 10 points per decade modified in frequency. EIS outcomes give acquaintance concerning the assessment of the protective capability of the new composite as a corrosion protection film. Figure 8a–d represents the Nyquist impedance plots acquired for PNMPY-1SSD/P2MT coatings of the brass substrate and for uncoated brass in sulfuric acid environments.

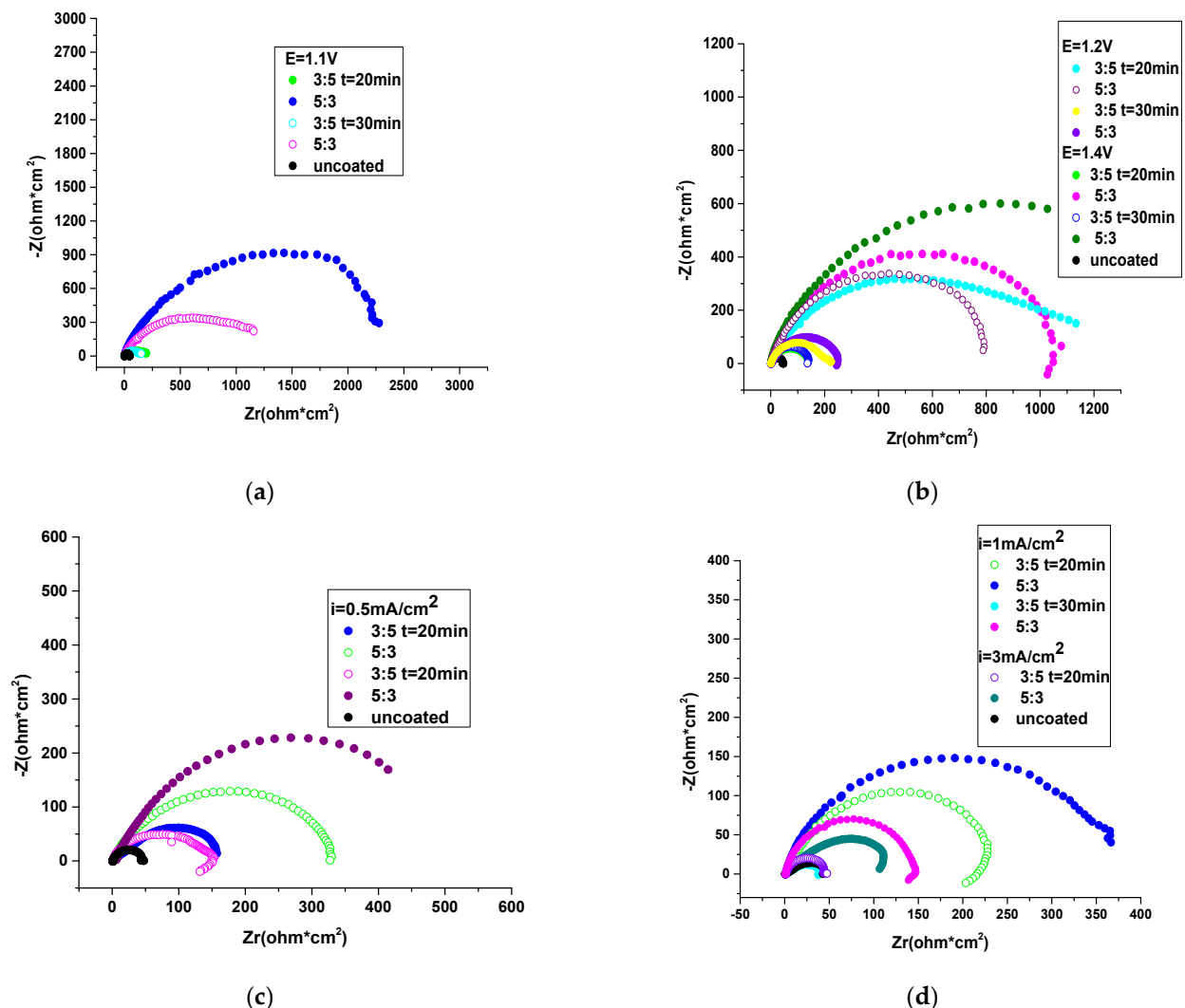


**Figure 8.** Nyquist plots for uncoated brass and PNMPY-1SSD/P2MT coated specimens by potentiostatic at (a) 1.1 V, (b) at 1.2 V and at 1.4 V and galvanostatic (c) at 0.5 mA/cm<sup>2</sup> and (d) at 1 mA/cm<sup>2</sup> and 3 mA/cm<sup>2</sup> practices at different molar ratios for PNMPY-1SSD and P2MT.

As shown in Figure 8, the Nyquist plots for the brass sample exhibited a little capacitive loop, representing that the charge transfer process was predominant during the corrosion reaction. Nyquist graphs (Figure 8a–d) for PNMPY-1SSD/P2MT coated on brass substrate

show only one semicircle, which is typical for a charge transfer mechanism. Therefore, the diameters of the capacitance loops by the coatings are larger than those of bare brass, and the sizes of these loops rise once the coatings are improved, proposing that these PNMPY-1SSD/P2MT coatings have higher shielding (inhibitory) characteristics on the brass sample in an acid environment. It is evident from the Nyquist diagrams that the impedance response of brass was notably modified by the electrochemical deposition of the coverings, suggesting that the acquired protective film has been established by the application of the PNMPY-1SSD/P2MT composite. Additionally, these capacitive loops are not explicit semicircles, and this aspect is attributed to frequency dispersion, attributed in particular to the roughness and inhomogeneities of the sample surface. Figure 8 shows that the diameters of the capacitance loops for coatings made at 1.1 V, 1.2 V, and 1.4 V potential applied and at 0.5 mA/cm<sup>2</sup> and at 1 mA/cm<sup>2</sup> current density at 5:3, 3:5, molar ratio, (deposited time 20 and 30 min) are higher compared to this bare brass, assuming a meaningful protective effect for the brass specimen in corrosive media. It can be remarked in Figure 8 that the diameters of the capacitance loops of PNMPY-1SSD/P2MT coatings acquired by potentiostatic procedure at 1.1 V and 1.4 V potential applied (in molar ratio at 5:3 and 3:5) are larger than those performed by potentiostatic technique at 0.5 mA/cm<sup>2</sup> and 1 mA/cm<sup>2</sup> current densities and as an effect the protection efficacy of this coating is higher.

It can be said from Figure 8 and Tables 4 and 5 that the PNMPY-1SSD/P2MT coatings acted as an efficient physical barrier that hindered the admission of the aggressive ions into the coatings, diminishing the charge transfer and, as a result, prevented the corrosion process. The Bode diagrams of PNMPY-1SSD/P2MT coating (Figure 9) showed that the impedance modulus, at low frequencies, raises with the increasing enhancement of this composite, designating that the deposition of the protective film of composite enlarges the anti-corrosion protection of the brass specimen investigated in an acid environment. From Figure 9, it is evident that bare brass shows one time constant approximately at a phase angle of 55° at medium and low frequencies, indicating an inductive behavior by attenuated diffusive tendency. From Figure 9, it can be noted that the existence of composite coatings on the diagram phase angle versus the frequency logarithm introduces a maximum very well caused at a phase angle of appraising 75–80°. Therefore, under these conditions, the covered specimens have good capacitive comportment in accordance with the Nyquist plots and experimental measurements obtained by the potentiodynamic polarization procedure. The increase in Zmod denotes greater protective ability, and it is clear that Zmod rises when coverage is enhanced. A higher Zmod induces superior protection efficiency. The assessment of the impedance tests were highlighted by fitting the data to the appropriate, equivalent circuit shown in Figure 10 and the varied impedance parameters as the solution resistance (Rs), the resistance of coating (Rf), the charge transfer resistance (Rct), the capacitance of coating (Cf), the capacitance of double layer (Cdl) and protection effectiveness have been presented in Tables 4–6. In this study, an equivalent circuit model has been proposed in the developed frequency range in order to fit and consider the EIS data obtained. In this case, the constant phase element, CPE, is exposed in the circuit instead of a pure double-layer capacitor (Cdl) to give a more accurate fit. The CPE is used to constitute the deformation of the capacitance semicircle, which assigns the heterogeneity of the area from surface roughness and impurities. The impedance of CPE can be considered as  $Z_{CPE} = Y_0^{-1} (j\omega)^{-n}$ , where  $\omega$  is the angular frequency,  $j$  is the imaginary number ( $j^2 = -1$ ),  $Y_0$  is the amplitude appropriate to capacitance, and  $n$  is the phase shift. The appraisal of the  $n$  provides characteristics about the stage of inhomogeneity of the metallic zone [28–34]. The larger value of the  $n$  is related to the reduced roughness of the zone, i.e., the inhomogeneity of the area is diminished. The CPE can be resistance when  $n = 0$ ,  $Y_0 = R$ , capacitance as  $n = 1$  ( $Y_0 = C$ ), and inductance when  $n = -1$  ( $Y_0 = 1/L$ ) or Warburg impedance as  $n = 0.5$  ( $Y_0 = W$ ) instituted at the assessment of  $n$  [30–36].

The EIS data denote that the charge transfer resistance Rct increased and the double layer capacitance Cdl lowered by composite coatings. The experimental results show that with the growth of Rct with the PNMPY-1SSD/P2MT consolidated layers, the protection

performance increases considerably, which indicates that the coating reveals the successful corrosion protection of the brass specimen. The lessening of Cdl may be feasible by decreasing the local dielectric constant and/or increasing the thickness of the electrical double layer as a result of the fact that the appearance of the composite acts by adsorption at the substrate/solution interface.

**Table 4.** Electrochemical parameters of uncoated and coated brass sample in 0.5 M sulfuric acid solutions at 25 °C.

The System PNMPY-1SSD/P2MT/Brass	Rs (ohm·cm <sup>2</sup> )	Q-Yo (S·s <sup>-n</sup> ·cm <sup>-2</sup> )	Q-n	Rf (ohm·cm <sup>2</sup> )	Q-Yo (S·s <sup>-n</sup> ·cm <sup>-2</sup> )	Q-n	Rct (ohm·cm <sup>2</sup> )	X
Brass + 0.5 M H <sub>2</sub> SO <sub>4</sub>	1.18	0.00023	0.95	4	0.00038	0.88	44	2.447 × 10 <sup>-3</sup>
PNMPY-1SSD/P2MT 1.1 V 3:5 molar ratio, t = 20 min	0.86	0.00032	0.88	74	0.00094	0.62	560	1.369 × 10 <sup>-3</sup>
PNMPY-1SSD/P2MT 1.1 V 5:3 molar ratio, t = 20 min	1.453	0.00004	0.88	505	0.000057	0.69	2116	4.51 × 10 <sup>-3</sup>
PNMPY-1SSD/P2MT 1.1 V 3:5 molar ratio, t = 30 min	0.81	0.0013	0.78	15	0.00108	0.6	140	5.802 × 10 <sup>-3</sup>
PNMPY-1SSD/P2MT 1.1 V 5:3 molar ratio, t = 30 min	0.87	0.00016	0.88	149	0.00047	0.61	1123	1.28 × 10 <sup>-3</sup>
PNMPY-1SSD/P2MT 1.2 V 3:5 molar ratio, t = 20 min	1.4	0.000043	0.92	18	0.00041	0.66	1120	1.731 × 10 <sup>-3</sup>
PNMPY-1SSD/P2MT 1.2 V 5:3 molar ratio, t = 20 min	1.44	0.000042	0.88	641	0.000049	0.77	1829	2.008 × 10 <sup>-3</sup>
PNMPY-1SSD/P2MT 1.2 V 3:5 molar ratio, t = 30 min	1.03	0.00034	0.83	46	0.00001	0.96	163	3.027 × 10 <sup>-3</sup>
PNMPY-1SSD/P2MT 1.2 V 5:3 molar ratio, t = 30 min	0.95	0.000045	0.98	16	0.00052	0.81	212	5.871 × 10 <sup>-4</sup>
PNMPY-1SSD/P2MT 1.4 V 3:5 molar ratio, t = 20 min	1.02	0.00146	0.81	12	0.00087	0.89	140	3.312 × 10 <sup>-3</sup>
PNMPY-1SSD/P2MT 1.4 V 5:3 molar ratio, t = 20 min	1.21	0.00019	0.90	226	0.00017	0.75	880	3.280 × 10 <sup>-3</sup>
PNMPY-1SSD/P2MT 1.4 V 3:5 molar ratio, t = 30 min	0.99	0.00061	0.87	15	0.00117	0.86	150	3.930 × 10 <sup>-3</sup>
PNMPY-1SSD/P2MT 1.4 V 5:3 molar ratio, t = 30 min	0.73	0.00317	0.74	54	0.0019	0.83	227	4.747 × 10 <sup>-4</sup>

**Table 5.** Electrochemical parameters of uncoated and coated brass sample in 0.5 M sulfuric acid solutions at 25 °C.

The System PNMPY-1SSD/P2MT/Brass	Rs (ohm·cm <sup>2</sup> )	Q-Yo (S·s <sup>-n</sup> ·cm <sup>-2</sup> )	Q-n	Rf (ohm·cm <sup>2</sup> )	Q-Yo (S·s <sup>-n</sup> ·cm <sup>-2</sup> )	Q-n	Rct (ohm·cm <sup>2</sup> )	X
Brass + 0.5 M H <sub>2</sub> SO <sub>4</sub>	1.18	0.00023	0.95	4	0.00038	0.88	44	2.447 × 10 <sup>-3</sup>
PNMPY-1SSD/P2MT 1 mA/cm <sup>2</sup> 3:5 molar ratio, t = 20 min	0.77	0.00042	0.87	89	0.00039	0.82	233	8.044 × 10 <sup>-3</sup>
PNMPY-1SSD/P2MT 1 mA/cm <sup>2</sup> 5:3 molar ratio, t = 20 min	1.19	0.00044	0.86	372	0.0218	0.76	6118	7.432 × 10 <sup>-4</sup>
PNMPY-1-DSS/PTPH 1 mA/cm <sup>2</sup> 3:5 molar ratio, t = 30 min	0.89	0.00303	0.62	110	0.01003	0.96	226	2.88 × 10 <sup>-3</sup>
PNMPY-1SSD/P2MT 1 mA/cm <sup>2</sup> 5:3 molar ratio, t = 30 min	0.79	0.00058	0.82	54	0.00061	0.74	129	4.336 × 10 <sup>-3</sup>
PNMPY-1SSD/P2MT 0.5 mA/cm <sup>2</sup> 3:5 molar ratio, t = 20 min	0.98	0.00109	0.76	35	0.00259	0.78	155	1.088 × 10 <sup>-3</sup>
PNMPY-1SSD/P2MT 0.5 mA/cm <sup>2</sup> 5:3 molar ratio, t = 20 min	1.10	0.00018	0.87	60	0.00170	0.74	101	3.082 × 10 <sup>-3</sup>
PNMPY-1SSD/P2MT 0.5 mA/cm <sup>2</sup> 3:5 molar ratio, t = 30 min	1.23	0.00054	0.86	159	0.00042	0.85	184	3.039 × 10 <sup>-3</sup>
PNMPY-1SSD/P2MT 0.5 mA/cm <sup>2</sup> 5:3 molar ratio, t = 30 min	1.46	0.00088	0.72	72	0.00243	0.83	645	2.803 × 10 <sup>-3</sup>
PNMPY-1SSD/P2MT 3 mA/cm <sup>2</sup> 3:5 molar ratio, t = 20 min	0.77	0.00059	0.78	36	0.00304	0.65	143	1.584 × 10 <sup>-3</sup>
PNMPY-1SSD/P2MT 3 mA/cm <sup>2</sup> 5:3 molar ratio, t = 20 min	0.87	0.00041	0.79	45	0.0031	0.71	104	2.881 × 10 <sup>-3</sup>

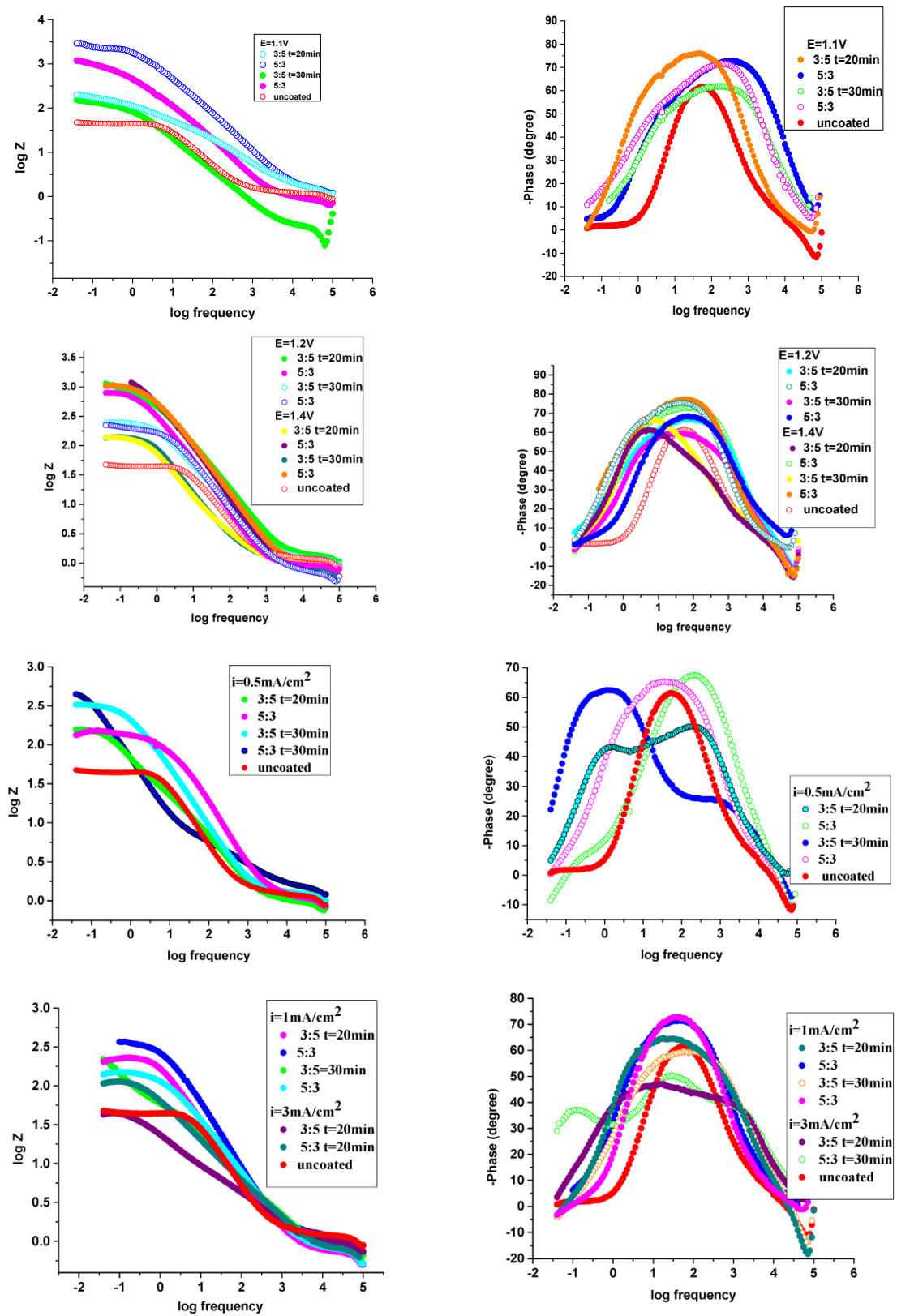


Figure 9. Bode graphs for uncoated brass and PNMPY-1SSD/P2MT coated specimens by potentiostatic and galvanostatic practices at different molar ratios for PNMPY-1SSD and P2MT.

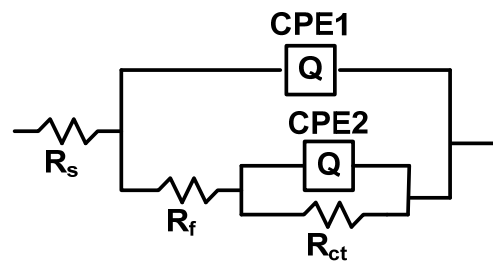


Figure 10. Equivalent circuit.

Table 6. Electrochemical parameters of coated and uncoated brass sample in 0.5 M sulfuric acid solutions at 25 °C at different immersion times.

The System PNMPY-1SSD/P2MT/Brass	$R_s$ (ohm·cm <sup>2</sup> )	Q-Yo (S·s <sup>-n</sup> ·cm <sup>-2</sup> )	Q-n	$R_f$ (ohm·cm <sup>2</sup> )	Q-Yo (S·s <sup>-n</sup> ·cm <sup>-2</sup> )	Q-n	$R_{ct}$ (ohm·cm <sup>2</sup> )	$\chi$
Brass + 0.5 M H <sub>2</sub> SO <sub>4</sub>	1.18	0.00023	0.95	4	0.00036	0.88	44	$2.447 \times 10^{-3}$
PNMPY-1SSD/P2MT 1.1 V 3:5 molar ratio, t = 20 min 0 h	1.45	$4.07 \times 10^{-5}$	0.88	505	0.000057	0.69	2116	$2.773 \times 10^{-3}$
PNMPY-1SSD/P2MT 1.1 V 3:5 molar ratio, t = 20 min 24 h	1.05	$5.58 \times 10^{-5}$	0.88	343	0.00017	0.62	1518	$4.514 \times 10^{-3}$
PNMPY-1SSD/P2MT 1.1 V 3:5 molar ratio, t = 20 min 48 h	1.02	$7.138 \times 10^{-5}$	0.89	39	0.00036	0.61	2357	$1.756 \times 10^{-3}$
PNMPY-1SSD/P2MT 1.1 V 3:5 molar ratio, t = 20 min 72 h	1.01	0.00012	0.88	29	0.00049	0.59	1909	$2.585 \times 10^{-3}$
PNMPY-1SSD/P2MT 1.1 V 3:5 molar ratio, t = 20 min 96 h	1.03	0.00091	0.73	32	0.000043	0.93	794	$6.557 \times 10^{-4}$
PNMPY-1SSD/P2MT 1.1 V 3:5 molar ratio, t = 20 min 120 h	1.13	0.00127	0.74	27	0.00018	0.87	670	$2.500 \times 10^{-3}$
PNMPY-1SSD/P2MT 1.1 V 3:5 molar ratio, t = 20 min 144 h	1.12	0.00136	0.73	24	0.00012	0.92	646	$2.603 \times 10^{-3}$
PNMPY-1SSD/P2MT 1.4 V 5:3 molar ratio, t = 30 min 0 h	0.73	0.00317	0.74	54	0.0019	0.83	227	$4.747 \times 10^{-4}$
PNMPY-1SSD/P2MT 1.4 V 5:3 molar ratio, t = 30 min 48 h	0.76	0.00228	0.80	32	0.0043	0.87	263	$2.321 \times 10^{-3}$
PNMPY-1SSD/P2MT 1.4 V 5:3 molar ratio, t = 30 min 72 h	0.77	0.0028	0.70	30	0.0059	0.90	293	$2.956 \times 10^{-3}$
PNMPY-1SSD/P2MT 1.4 V 5:3 molar ratio, t = 30 min 96 h	0.63	0.00295	0.65	26	0.0082	0.85	304	$1.405 \times 10^{-3}$
PNMPY-1SSD/P2MT 1.4 V 5:3 molar ratio, t = 30 min 144 h	0.61	0.00301	0.64	22	0.0099	0.85	294	$1.755 \times 10^{-3}$

It can be seen from Figures 11 and 12 that the dimension of the capacitance loops in the existence of PNMPY-1SSD/P2MT coatings decreases slightly with the rising immersion period. Additionally, for immersion time from 96 to 144 (168) h, a slight diminution in protection efficiency of this composite is evident, which involves the diffusion of corrosive ions (SO<sub>4</sub><sup>2-</sup>) in the coated surface. These experimental EIS results (Figures 11 and 12 and Table 6) establish the performance of PNMPY-1SSD/P2MT coating in impeding the migration of aggressive agents (SO<sub>4</sub><sup>2-</sup>) on the surface above a long immersion time.

In this study, the PNMPY-1SSD/P2MT coating electrochemically deposited over the substrate of the brass specimen illustrates a protective film on the brass electrode. The Nyquist and Bode diagrams (Figures 7–12, Tables 4–6) imply that the effect of corrosion has been prevented by the electrodeposition of the PNMPY-1SSD/P2MT composites and this fact is achieved as a diffusion barrier by a charge transfer mechanism.

### 3.5. SEM Examination

Using scanning electron microscopy (SEM), the morphological structure of the PNMPY-1SSD/P2MT polymer composite coatings accomplished onto a brass substrate has been considered. SEM micrographs of PNMPY-1SSD/P2MT coatings electrochemically deposited under differing conditions on brass samples are shown in Figure 13. These micrographs

present a black film of the PNMPY-1SSD/P2MT performed by potentiostatic and galvanostatic practices indicating that the coated composite has been made.

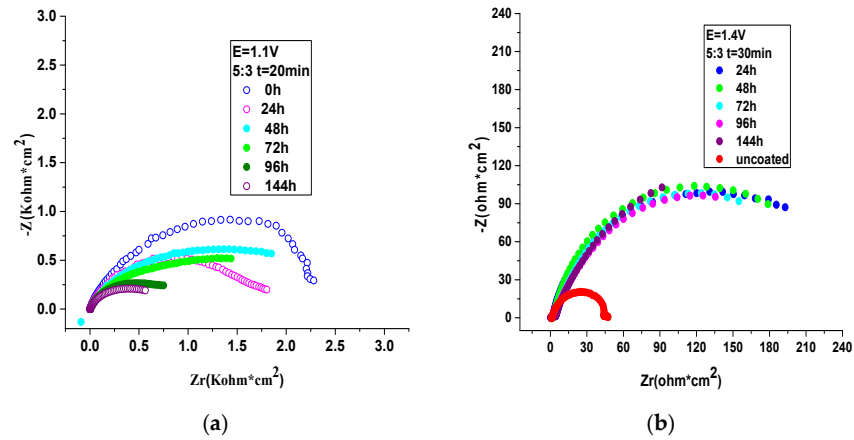


**Figure 11.** Nyquist plots for uncoated brass and PNMPY-1SSD/P2MT coated specimens by electrochemical deposition practices at (a)  $E = 1.1\text{ V}$  and (b) at  $E = 1.4\text{ V}$  and to different molar ratios for PNMPY-SSD and P2MT and at different immersion times.

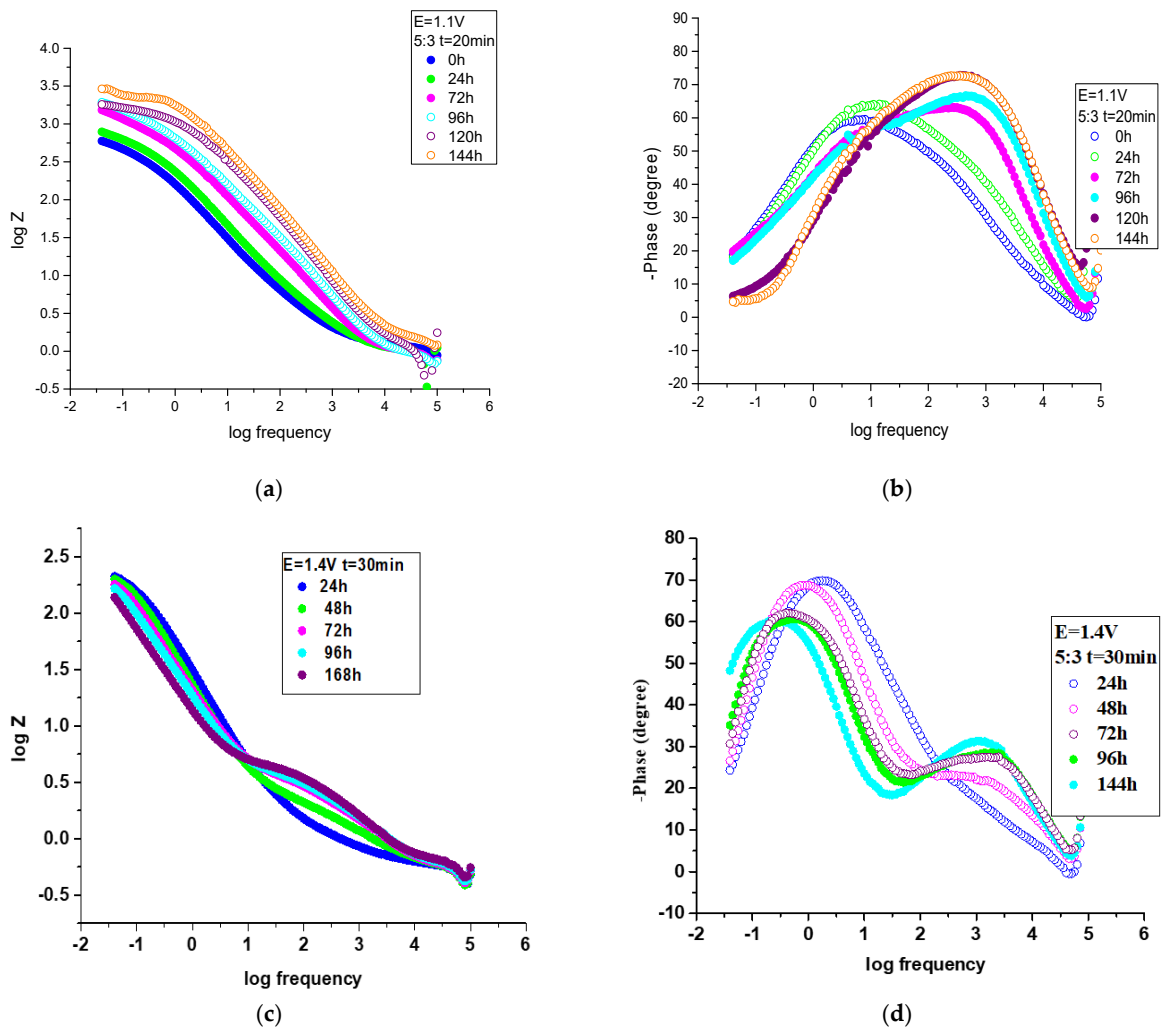
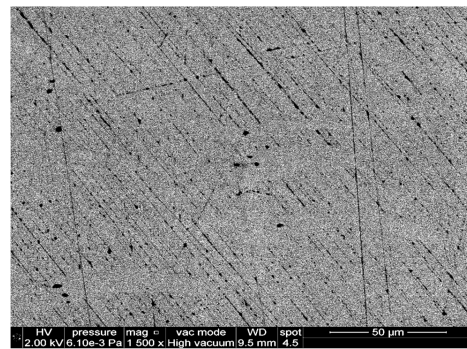
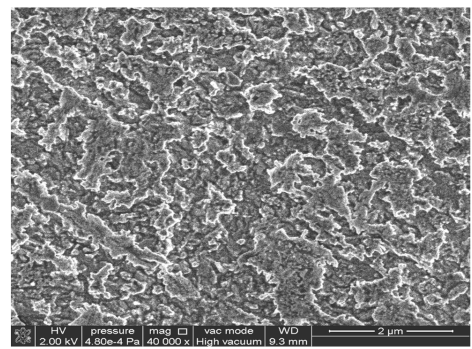


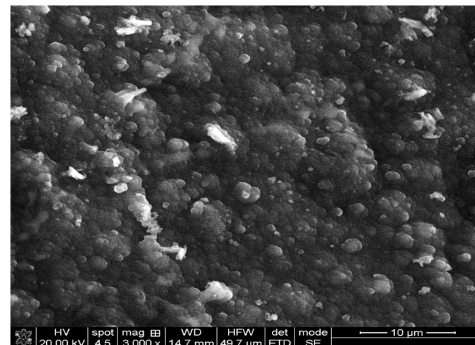
**Figure 12.** Bode diagrams for uncoated brass and PNMPY-1SSD/P2MT coated specimens by electrochemical deposition practices at (a,b) at  $E = 1.1\text{ V}$  and (c,d) at  $E = 1.4\text{ V}$  at different molar ratios for PNMPY-1SSD and P2MT at different immersion times.



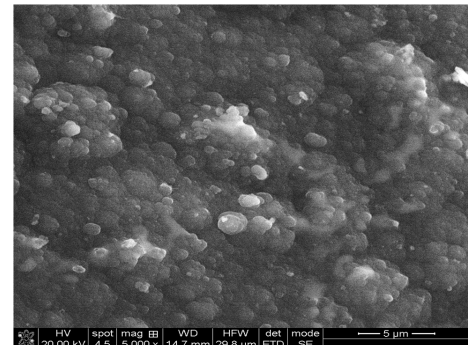
(a)



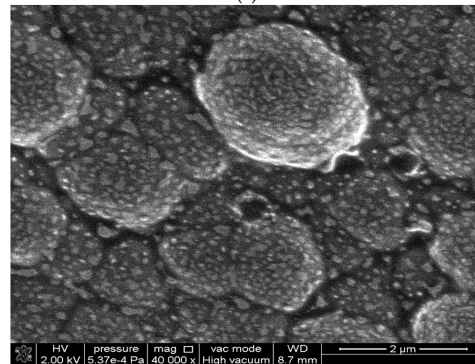
(b)



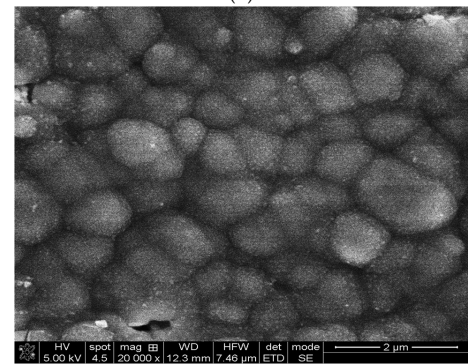
(c)



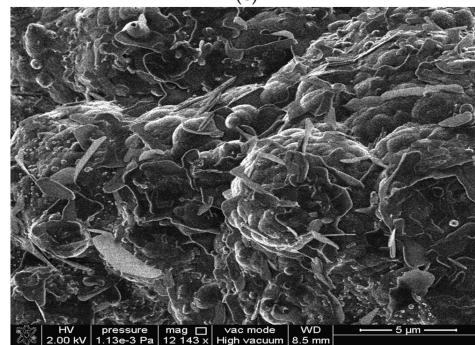
(d)



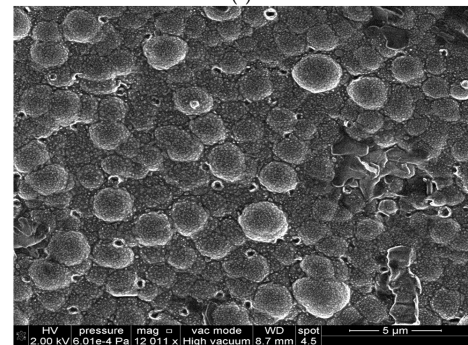
(e)



(f)



(g)



(h)

Figure 13. Cont.

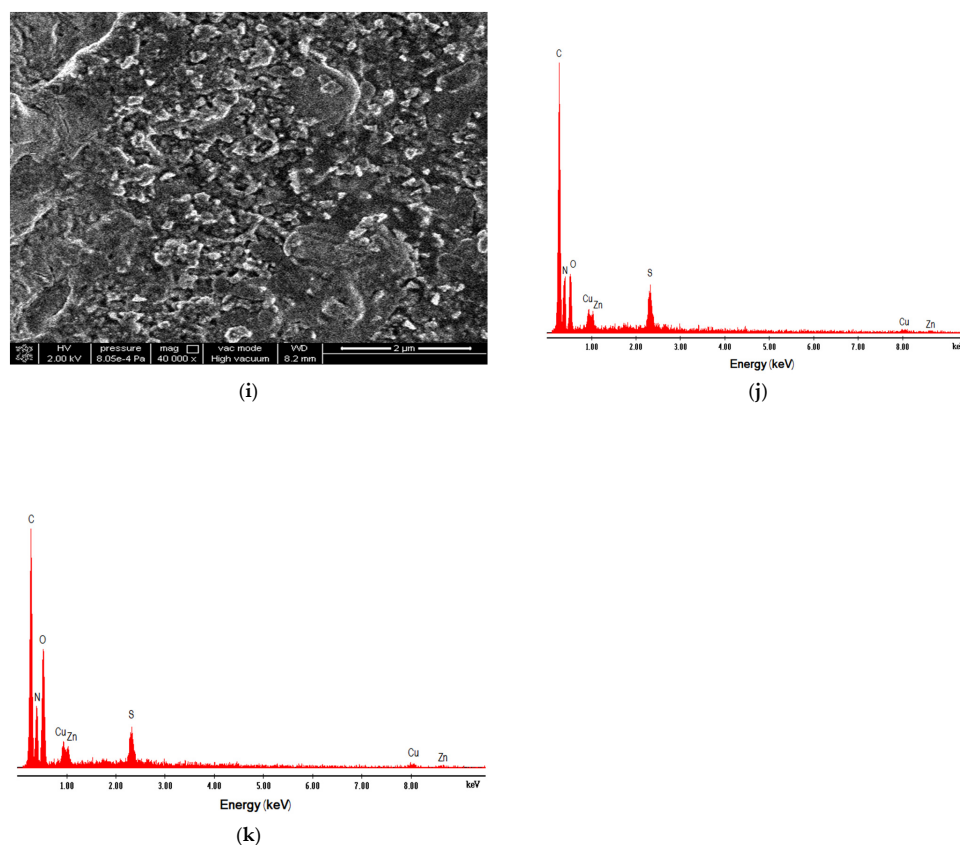


**Figure 13.** SEM micrographs of brass sample coated with PNMPY-1SSD/P2MT, (a) uncoated brass, (b) brass in 0.5 M  $H_2SO_4$ , (c) at 1.2 V, (d) 1.4 V, (e) at 0.5  $mA/cm^2$ , (f) 1  $mA/cm^2$  in 5:3, 3:5 molar ratio, and (g–i) after 96 h, 120 h, and 144 h immersion period in 0.5 M sulfuric acid, (j,k) the EDS spectra PNMPY-1SSD/P2MT/brass.

As shown in Figure 12a,b brass specimen uncoated and brass in 0.5 M  $H_2SO_4$ , and from Figure 13c–i, the PNMPY-1SSD/P2MT coating has a uniform shape of cauliflower form with a little globular micro-structure allocated dense and adherent onto the brass surface, which is considered adequate in the literature [4,28–31]. The grains are 5  $\mu m$  in size with an average thickness of 50  $\mu m$ . These micrographs exhibited a uniform layer to be achieved over the brass substrate, and the properties of this coating are so qualitative that no cracks are observed on the coating. The dopant anionic surfactant (1SSD) incorporated in conducting polymers affects both the electropolymerization procedure and also the properties of the resulting coating [33–38,40–43]. The higher surface coverage and higher adsorption effect also explained the better anti-corrosion protection effectiveness of the composite layers. EDS examination of the PNMPY-1SSD/P2MT coated brass was performed, and the spectra were indicated in Figure 13j,k). The companion of the composite layer on the brass substrate is noticed from the peaks of C, N, O, and S components in the EDS spectrum. These results are in agreement with the FTIR spectrum of composite coating, where the anionic surfactant and oxalate ions are present in the polymer matrix. Subsequent to the immersion period from 0 and 144 h (168 h) in 0.5 M sulfuric acid solution, the evident change in the surface morphology of the coating appeared by the electrochemical experiments. The PNMPY-1SSD/P2MT coating performed by potentiostatic practice (at 1.1 V) exposed a non-damaging topography after 144 h of immersion in the corrosive environment (Figure 13g), further establishing their best protective capability. It can be remarked from the micrographs: Figure 13h,i which shows the diffusion of corrosive agents  $SO_4^{2-}$  in the coating substrate.

#### 4. Conclusions

Homogeneous, compact, uniform, and adherent PNMPY-1SSD/P2MT composite coatings were successfully electrochemically deposited on the brass specimen were made using the potentiostatic and galvanostatic practice at various potentials and current densities in  $\text{H}_2\text{C}_2\text{O}_4$  environment.

The electrochemical experiments establish that the PNMPY-1SSD/P2MT behaves as a protective film on brass in sulfuric acid media.

The electropolymerization practice used to obtain composite coating is most appropriate, quite simple, and cheap.

The anti-corrosion protection behavior of the PNMPY-1SSD/P2MT coating electrochemical deposited in the optimal conditions were considered in 0.5 M sulfuric acid solution by potentiodynamic polarization and EIS procedures.

The corrosion appraises of this PNMPY-1SSD/P2MT composite coated brass substrate are approximated to be ~9 times lower than brass, and the protection performance of this coating is over 90%.

The corrosion protection features follow the succession: PNMPY-1SSD/P2MT to:

$1.1 \text{ V} > 1.4 \text{ V} > 1.2 \text{ V} > 0.5 \text{ mA/cm}^2 > 1 \text{ mA/cm}^2 > 3 \text{ mA/cm}^2$  because the existence of these coatings causes an appreciable reduction in the corrosion mechanism.

Exploration of FT-IR spectra evidence that the PNMPY-1SSD/P2MT composite is formed on the brass electrode.

The SEM micrographs of PNMPY-1SSD/P2MT coating accomplished on brass are dense, homogeneous, and adherent over the brass substrate, and the attribute of the coating is of the best quality.

The higher surface coverage and higher adsorption effect also explained the better anti-corrosion protection performance of the composite coatings.

Due to the enhanced physical barrier effect, the coating surface is uniform and homogeneous; through low porosity and superior protective ability, the PNMPY-1SSD/P2MT coatings were more corrosion resistant.

The PNMPY-1SSD/P2MT coating accomplished by the potentiostatic method (at 1.1V) displayed a non-damaging topography after 96 h of immersion in the corrosive solution, further confirming their superior protective ability.

The PNMPY-1SSD/P2MT coatings were performed at 1.1 V and 1.4 V potential applied, and to  $0.5 \text{ mA/cm}^2$  and  $1 \text{ mA/cm}^2$  current density in molar ratio at 5:3 and 3:5 NMPY-1SSD:2MT at 20 min and 30 min permitted polymer exhibited excellent corrosion protection performance than the coating acquired at 1.2 V potential applied and  $3 \text{ mA/cm}^2$  current density under same conditions.

It was clear that the composite coatings impede the aggression of the corrosive factor ( $\text{H}_2\text{SO}_4$ ) on the brass surface, and the new composite PNMPY-1SSD/P2MT obtained by this procedure is encouraging and may lead to manufacturing practices for the protection of the metallic materials against corrosion mechanism.

**Author Contributions:** Conceptualization F.B.; methodology, F.B.; software, F.B.; validation, F.B.; formal analysis F.B. and S.P.; investigation, F.B.; resources, F.B.; data curation, F.B. and S.P.; writing—original draft preparation, F.B.; writing—review and editing, F.B.; visualization, F.B.; supervision F.B.; project administration, F.B.; funding acquisition, F.B. All authors have read and agreed to the published version of the manuscript.

**Funding:** This research received no external funding.

**Institutional Review Board Statement:** Not applicable.

**Informed Consent Statement:** Not applicable.

**Data Availability Statement:** Not applicable.

**Conflicts of Interest:** The authors declare no conflict of interest.

## References

1. Song, L.; Gao, Z.; Sun, Q.; Chu, G.; Shi, H.; Xu, N.; Li, Z.; Hao, N.; Zhang, X.; Ma, F.; et al. Corrosion protection performance of a coating with 2-aminino-5-mercato-1,3,4-thiadizole-loaded hollow mesoporous silica on copper. *Prog. Org. Coat.* **2023**, *175*, 107331. [[CrossRef](#)]
2. Liao, F.-Q.; Chen, Y.-C. Siloxane-based epoxy coatings through cationic photopolymerization for corrosion protection. *Prog. Org. Coat.* **2023**, *174*, 107235. [[CrossRef](#)]
3. Ramezanzadeh, M.; Ramezanzadeh, B.; Mahdavian, M. Epoxy-zinc phosphate coating dual barrier/active corrosion prevention properties improvement via polyaniline modified lamellar kaolinite (Ka@PANI) hybrid-pigment. *Prog. Org. Coat.* **2022**, *172*, 107132. [[CrossRef](#)]
4. Branzoi, F.; Branzoi, V. Enzymatic electrode obtained by immobilizing of urease into a nanocomposite film based on conducting polymers and different additives. *Int. J. Polym. Mater. Polym. Biomater.* **2014**, *63*, 549–556. [[CrossRef](#)]
5. Gallegos-Melgar, A.; Serna, S.A.; Lázaro, I.; Gutiérrez-Castañeda, J.; Mercado-Lemus VArco-Gutierrez, H.H.; Hernández-Hernández, M.; Porcayo-Calderón Jan Mayen, J.; Del Angel Monroy, M. Potentiodynamic Polarization Performance of a Novel Composite Coating System of Al<sub>2</sub>O<sub>3</sub>/Chitosan-Sodium Alginate, Applied on an Aluminum AA6063 Alloy for Protection in a Chloride Ions Environment. *Coatings* **2020**, *10*, 45. [[CrossRef](#)]
6. Xie, J.; Lu, Z.; Zhou, K.; Li, C.; Ma, J.; Wang, B.; Xu, K.; Cui, H.; Liu, J. Researches on corrosion behaviors of carbon steel/copper alloy couple under organic coating in static and flowing seawater. *Prog. Org. Coat.* **2022**, *166*, 106793. [[CrossRef](#)]
7. Fan, H.; Li, S.; Zhao, Z.; Wang, H.; Shi, Z.; Zhang, L. Inhibition of brass corrosion in sodium chloride solutions by self-assembled silane films. *Corros. Sci.* **2011**, *53*, 4273–4281. [[CrossRef](#)]
8. Zhang, J. A Zhu Study on the synthesis of PANI/CNT nanocomposite and its anticorrosion mechanism in waterborne coatings. *Prog. Org. Coat.* **2021**, *159*, 106447. [[CrossRef](#)]
9. Branzoi, F.; Băran, A. The inhibition effect of some organic compounds on corrosion of brass and carbon steel in aggressive medium. *Int. J. Electrochem. Sci.* **2019**, *14*, 2780–2803. [[CrossRef](#)]
10. Liu, Z.; Fan, B.; Zhao, J.; Yang, B.; Zheng, X. Benzothiazole derivatives-based supramolecular assemblies as efficient corrosion inhibitors for copper in artificial seawater: Formation, interfacial release and protective mechanisms. *Corros. Sci.* **2023**, *212*, 110957. [[CrossRef](#)]
11. Damej, M.; Chebabe, D.; Abbout, S.; Erramli, H.; Oubair, A.; Hajjaji, N. Corrosion inhibition of brass 60Cu–40Zn in 3% NaCl solution by 3-amino-1,2,4-triazole-5-thiol. *Heliyon* **2020**, *6*, e04026. [[CrossRef](#)] [[PubMed](#)]
12. Chaudhari, S.; Gaikwad, A.; Patil, P. Poly(o-anisidine) coatings on brass: Synthesis, characterization and corrosion protection. *Curr. Appl. Phys.* **2009**, *9*, 206–218. [[CrossRef](#)]
13. Fan, H.-Q.; Xia, D.-H.; Li, M.-C.; Li, Q. Self-assembled (3-mercaptopropyl)trimethoxysilane film modified with La<sub>2</sub>O<sub>3</sub> nanoparticles for brass corrosion protection in NaCl solution. *J. Alloys Compd.* **2017**, *702*, 60–67. [[CrossRef](#)]
14. Patil, D.; Patil, P.P. Electrodeposition of poly(o-toluidine) on brass from aqueous salicylate solution and its corrosion protection performance. *J. Appl. Polym. Sci.* **2010**, *118*, 2084–2091. [[CrossRef](#)]
15. Fouda, A.; El-Dossoki, F.; Shady, I.A. Adsorption and corrosion inhibition behavior of polyethylene glycol on  $\alpha$ -brass alloy in nitric acid solution. *Green Chem. Lett. Rev.* **2018**, *11*, 67–77. [[CrossRef](#)]
16. Sun, Y.; Hu, C.; Cui, J.; Shen, S.; Qiu, H.; Li, J. Electrodeposition of polypyrrole coatings doped by benzenesulfonic acid-modified graphene oxide on metallic bipolar plates. *Prog. Org. Coat.* **2022**, *170*, 106995. [[CrossRef](#)]
17. Yılmaz, S.M.; Atun, G. Corrosion protection efficiency of the electrochemically synthesized polypyrrole-azo dye composite coating on stainless steel. *Prog. Org. Coat.* **2022**, *169*, 106942. [[CrossRef](#)]
18. Branzoi, F.; Băran, A.; Ludmila, A.; Alexandrescu, E. The inhibition action of some organic polymers on the corrosion carbon steel in acidic media. *Chem. Pap.* **2020**, *74*, 4315–4335. [[CrossRef](#)]
19. Zhang, Y. Strengthening, Corrosion and Protection of High-Temperature Structural Materials. *Coatings* **2022**, *12*, 1136. [[CrossRef](#)]
20. Zhai, Y.; Pan, K.; Zhang, E. Anti-Corrosive Coating of Carbon-Steel Assisted by Polymer-Camphor sulfonic Acid Embedded within Graphene. *Coatings* **2020**, *10*, 879. [[CrossRef](#)]
21. Sinapi, F.; Deroubaix, S.; Pirlot, C.; Delhalle, J.; Mekhalif, Z. Electrochemical evaluation of the corrosion protection of bi-dimensional organic films self-assembled onto brass. *Electrochim. Acta* **2004**, *49*, 2987–2996. [[CrossRef](#)]
22. Shinde, V.; Gaikwad, A.; Patil, P. Synthesis and characterization of corrosion protective poly(2,5-dimethylaniline) coatings on copper. *Appl. Surf. Sci.* **2006**, *253*, 1037–1045. [[CrossRef](#)]
23. Davoodi, A.; Honarbakhsh, S.; Farzi, G.A. Evaluation of corrosion resistance of polypyrrole/functionalized multi-walled carbon nanotubes composite coatings on 60Cu–40Zn brass alloy. *Prog. Org. Coat.* **2015**, *88*, 106–115. [[CrossRef](#)]
24. Özyılmaz, A.T.; Çolak, N.; Ozyılmaz, G.; Sangün, M.K. Protective properties of polyaniline and poly(aniline-co-o-anisidine) films electrosynthesized on brass. *Prog. Org. Coat.* **2007**, *60*, 24–32. [[CrossRef](#)]
25. Bazzaoui, M.; Martins, J.; Bazzaoui, E.; Martins, L.; Machnikova, E. Sweet aqueous solution for electrochemical synthesis of polypyrrole part 1B: On copper and its alloys. *Electrochimica Acta* **2007**, *52*, 3568–3581. [[CrossRef](#)]
26. González-Tejera, M.; García, M.; De La Blanca, E.S.; Redondo, M.; Raso, M.; Carrillo, I. Electrochemical synthesis of N-methyl and 3-methyl pyrrole perchlorate doped copolymer films. *Thin Solid Films* **2007**, *515*, 6805–6811. [[CrossRef](#)]
27. Herrasti, P.; Patil, P. Corrosion protective poly(o-ethoxyaniline) coatings on copper. *Electrochim. Acta* **2007**, *53*, 927–933.

28. Branzoi, F.; Brânzoi, V.; Musina, A. Fabrication and characterisation of conducting composite films based on conducting polymers and functionalised carbon nanotubes. *Surf. Interface Anal.* **2012**, *44*, 1076–1080. [[CrossRef](#)]
29. Duran, B.; Bereket, G. Cyclic Voltammetric Synthesis of Poly(*N*-methyl pyrrole) on Copper and Effects of Polymerization Parameters on Corrosion Performance. *Ind. Eng. Chem. Res.* **2012**, *51*, 5246–5255. [[CrossRef](#)]
30. Redondo, M.; de la Blanca, E.S.; García, M.; González-Tejera, M. Poly(*N*-methylpyrrole) electrodeposited on copper: Corrosion protection properties. *Prog. Org. Coat.* **2009**, *65*, 386–391. [[CrossRef](#)]
31. Ren, S.; Barkey, D. Electrochemically Prepared Poly(3-methylthiophene) Films for Passivation of 430 Stainless Steel. *J. Electrochem. Soc.* **1992**, *139*, 1021–1026. [[CrossRef](#)]
32. Branzoi, F.; Băran, A.; Petrescu, S. Evaluation of Corrosion Protection Performance of New Polymer Composite Coatings on Carbon Steel in Acid Medium by Electrodeposition Methods. *Coatings* **2021**, *11*, 903. [[CrossRef](#)]
33. Çakmakçı, İ.; Duran, B.; Duran, M.; Bereket, G. Experimental and theoretical studies on protective properties of poly (pyrrole-co-*N*-methyl pyrrole) coatings on copper in chloride media. *Corros. Sci.* **2013**, *69*, 252–261. [[CrossRef](#)]
34. He, C. Studies on Corrosion Behaviors of Q235 Steel Coated by the Polypyrrole Films Doped with different dopants. *Int. J. Electrochem. Sci.* **2020**, *15*, 2594–2603.
35. Rui, M.; Zhu, A. The synthesis and corrosion protection mechanisms of PANI/CNT nanocomposite doped with organic phosphoric acid. *Prog. Org. Coat.* **2021**, *153*, 106134. [[CrossRef](#)]
36. Martí, M.; Armelin, E.; Iribarren, J.I.; Alemán, C. Soluble polythiophenes as anticorrosive additives for marine epoxy paints. *Mater. Corros.* **2015**, *66*, 23–30. [[CrossRef](#)]
37. Branzoi, F.; Pahom, Z.; Nechifor, G. Corrosion protection of new composite polymer coating for carbon steel in sulfuric acid medium by electrochemical methods. *J. Adhes. Sci. Technol.* **2018**, *32*, 2364–2380. [[CrossRef](#)]
38. Fan, B.; Zhao, X.; Liu, Z.; Xiang, Y.; Zheng, X. Inter-component synergetic corrosion inhibition mechanism of Passiflora edulia Sims shell extract for mild steel in pickling solution: Experimental, DFT and reactive dynamics investigations. *Sustain. Chem. Pharm.* **2022**, *29*, 100821. [[CrossRef](#)]
39. Pauline, S.A.; Sahila, S.; Gopalakrishnan, C.; Nanjundan, S.; Rajendran, N. Synthesis, characterization and corrosion protection property of terpolymers derived from poly(MAn-co-MMA) containing benzimidazole derivative as pendant group. *Prog. Org. Coat.* **2011**, *72*, 443–452. [[CrossRef](#)]
40. Asan, G.; Asan, A.; Çelikkan, H. The effect of 2D-MoS<sub>2</sub> doped polypyrrole coatings on brass corrosion. *J. Mol. Struct.* **2020**, *1203*, 127318. [[CrossRef](#)]
41. Menkuer, M.; Ozkazanc, H. Anticorrosive polypyrrole/zirconium-oxide composite film prepared in oxalic acid and dodecylbenzene sulfonic acid mix electrolyte. *Prog. Org. Coatings* **2020**, *147*, 105815. [[CrossRef](#)]
42. Pekmeza, N.Ö.; Cinkillia, K.; Zeybekba, B. The electrochemical copolymerization of pyrrole and bithiophene on stainless steel in the presence of SDS in aqueous medium and its anticorrosive performance. *Prog. Org. Coat.* **2014**, *77*, 1277–1287. [[CrossRef](#)]
43. Gupta, D.K.; Neupane, S.; Singh, S.; Karki, N.; Yadav, A.P. The effect of electrolytes on the coating of polyaniline on mild steel by electrochemical methods and its corrosion behavior. *Prog. Org. Coat.* **2021**, *152*, 106127. [[CrossRef](#)]

**Disclaimer/Publisher's Note:** The statements, opinions and data contained in all publications are solely those of the individual author(s) and contributor(s) and not of MDPI and/or the editor(s). MDPI and/or the editor(s) disclaim responsibility for any injury to people or property resulting from any ideas, methods, instructions or products referred to in the content.